

Part 2. Three Primary Areas of Theoretical Chemistry

Chapter 5. An Overview of Theoretical Chemistry

In this Chapter, many of the basic concepts and tools of theoretical chemistry are discussed only at an introductory level and without providing much of the background needed to fully comprehend them. Most of these topics are covered again in considerably more detail in Chapters 6-8, which focus on the three primary sub-disciplines of the field. The purpose of the present Chapter is to give you an overview of the field that you will learn the details of in these later Chapters. It probably will mainly be of use to undergraduate students using this text to learn about theoretical chemistry; most graduate students and more senior scientists should be able to skip this Chapter or briefly glance through it.

5.1 What is Theoretical Chemistry About?

The science of chemistry deals with molecules including the radicals, cations, and anions they produce when fragmented or ionized. Chemists study isolated molecules (e.g., as occur in the atmosphere and in astronomical environments), solutions of molecules or ions dissolved in solvents, as well as solid, liquid, and plastic materials comprised of molecules. All such forms of molecular matter are what chemistry is about. Chemical science includes how to make molecules (synthesis), how to detect and quantitate them (analysis), how to probe their properties and the changes they undergo as reactions occur (physical).

5.1.1 Molecular Structure- bonding, shapes, electronic structures

One of the more fundamental issues chemistry addresses is molecular structure, which means how the molecule's atoms are linked together by bonds and what the inter-

atomic distances and angles are. Another component of structure analysis relates to what the electrons are doing in the molecule; that is, how the molecule's orbitals are occupied and in which electronic state the molecule exists. For example, in the arginine molecule shown in Fig. 5.1, a HOOC- carboxylic acid group (its oxygen atoms are shown in red) is linked to an adjacent carbon atom (yellow) which itself is bonded to an -NH_2 amino group (whose nitrogen atom is blue). Also connected to the α -carbon atom are a chain of three methylene $\text{-CH}_2\text{-}$ groups, a -NH- group, then a carbon atom attached both by a double bond to an imine -NH group and to an amino -NH_2 group.

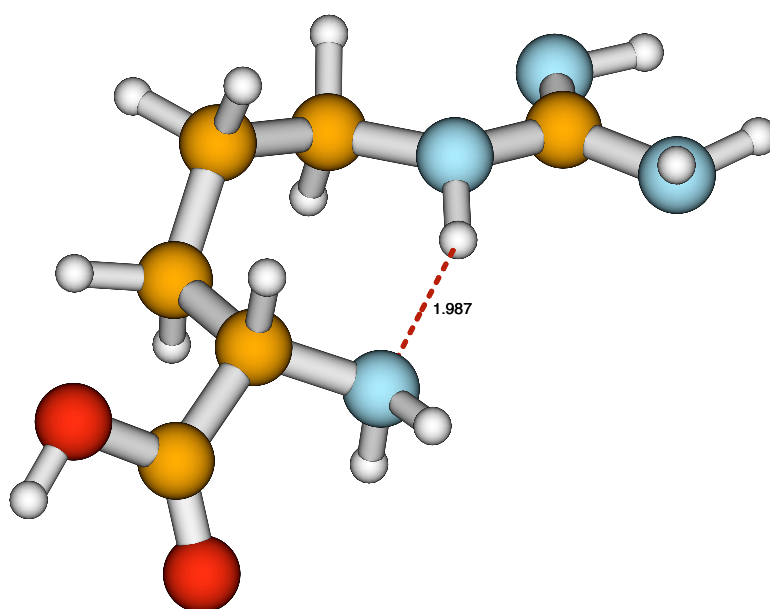


Figure 5.1 The arginine molecule in its non-zwitterion form with dotted hydrogen bond.

The connectivity among the atoms in arginine is dictated by the well known valence preferences displayed by H, C, O, and N atoms. The internal bond angles are, to a large extent, also determined by the valences of the constituent atoms (i.e., the sp^3 or sp^2 nature of the bonding orbitals). However, there are other interactions among the several functional groups in arginine that also contribute to its ultimate structure. In particular, the hydrogen bond linking the α -amino group's nitrogen atom to the -NH- group's

hydrogen atom causes this molecule to fold into a less extended structure than it otherwise might.

What does theory have to do with issues of molecular structure and why is knowledge of structure so important? It is important because the structure of a molecule has a very important role in determining the kinds of reactions that molecule will undergo, what kind of radiation it will absorb and emit, and to what active sites in neighboring molecules or nearby materials it will bind. A molecule's shape (e.g., rod like, flat, globular, etc.) is one of the first things a chemist thinks of when trying to predict where, at another molecule or on a surface or at a cell membrane, the molecule will fit and be able to bind and perhaps react. The presence of lone pairs of electrons (which act as Lewis base sites), of π orbitals (which can act as electron donor and electron acceptor sites), and of highly polar or ionic groups guide the chemist further in determining where on the molecule's framework various reactant species (e.g., electrophilic or nucleophilic or radical) will be most strongly attracted. Clearly, molecular structure is a crucial aspect of the chemists' toolbox.

How does theory relate to molecular structure? As we discussed in the Part 1 of this text, the Born-Oppenheimer approximation leads us to use quantum mechanics to predict the energy E of a molecule for any positions ($\{R_a\}$) of its nuclei, given the number of electrons N_e in the molecule (or ion). This means, for example, that the energy of the arginine molecule in its lowest electronic state (i.e., with the electrons occupying the lowest energy orbitals) can be determined for any location of the nuclei if the Schrödinger equation governing the movements of the electrons can be solved.

If you have not had a good class on how quantum mechanics is used within chemistry, I urge you to take the time needed to master Part 1. In those pages, I introduce the central concepts of quantum mechanics and I show how they apply to several very important cases including

- 1. electrons moving in 1, 2, and 3 dimensions and how these models relate to electronic structures of polyenes and to electronic bands in solids*
- 1. the classical and quantum probability densities and how they differ,*
- 2. time propagation of quantum wave functions,*

3. *the Hückel or tight-binding model of chemical bonding among atomic orbitals,*
4. *harmonic vibrations,*
5. *molecular rotations,*
6. *electron tunneling,*
7. *atomic orbitals' angular and radial characteristics,*
8. *and point group symmetry and how it is used to label orbitals and vibrations.*

You need to know this material if you wish to understand most of what this text offers, so I urge you to read Part 1 if your education to date has not yet adequately been exposed to it.

Let us now return to the discussion of how theory deals with molecular structure. We assume that we know the energy $E(\{R_a\})$ at various locations $\{R_a\}$ of the nuclei. In some cases, we denote this energy $V(R_a)$ and in others we use $E(R_a)$ because, within the Born-Oppenheimer approximation, the electronic energy E serves as the potential V for the molecule's vibrational motions. As discussed in Part 1, one can then perform a search for the lowest energy structure (e.g., by finding where the gradient vector vanishes $\partial E/\partial R_a = 0$ and where the second derivative or Hessian matrix ($\partial^2 E/\partial R_a \partial R_b$) has no negative eigenvalues). By finding such a local-minimum in the energy landscape, theory is able to determine a stable structure of such a molecule. The word stable is used to describe these structures not because they are lower in energy than all other possible arrangements of the atoms but because the curvatures, as given in terms of eigenvalues of the Hessian matrix ($\partial^2 E/\partial R_a \partial R_a$), are positive at this particular geometry. The procedures by which minima on the energy landscape are found may involve simply testing whether the energy decreases or increases as each geometrical coordinate is varied by a small amount. Alternatively, if the gradients $\partial E/\partial R_a$ are known at a particular geometry, one can perform searches directed downhill along the negative of the gradient itself. By taking a small step along such a direction, one can move to a new geometry that is lower in energy. If not only the gradients $\partial E/\partial R_a$ but also the second derivatives ($\partial^2 E/\partial R_a \partial R_a$) are known at some geometry, one can make a more intelligent step toward a geometry of lower energy. For additional details about how such geometry optimization searches are performed within

modern computational chemistry software, see Chapter 3 where this subject was treated in greater detail.

It often turns out that a molecule has more than one stable structure (isomer) for a given electronic state. Moreover, the geometries that pertain to stable structures of excited electronic state are different than those obtained for the ground state (because the orbital occupancy and thus the nature of the bonding is different). Again using arginine as an example, its ground electronic state also has the structure shown in Fig. 5.2 as a stable isomer. Notice that this isomer and that shown earlier have the atoms linked together in identical manners, but in the second structure the α -amino group is involved in two hydrogen bonds while it is involved in only one in the former. In principle, the relative energies of these two geometrical isomers can be determined by solving the electronic Schrödinger equation while placing the constituent nuclei in the locations described in the two figures.

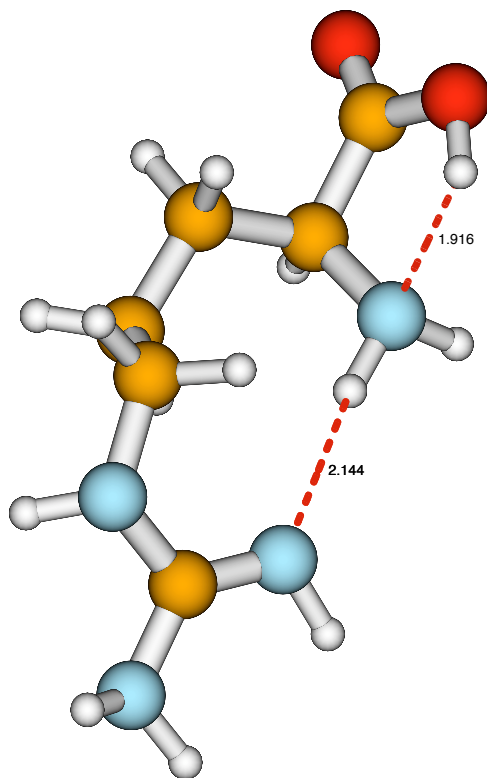


Figure 5.2 Another stable structure for the arginine molecule.

If the arginine molecule is excited to another electronic state, for example, by

promoting a non-bonding electron on its C=O oxygen atom into the neighboring C-O π^* orbital, its stable structures will not be the same as in the ground electronic state. In particular, the corresponding C-O distance will be longer than in the ground state, but other internal geometrical parameters may also be modified (albeit probably less so than the C-O distance). Moreover, the chemical reactivity of this excited state of arginine will be different than that of the ground state because the two states have different orbitals available to react with attacking reagents.

In summary, by solving the electronic Schrödinger equation at a variety of geometries and searching for geometries where the gradient vanishes and the Hessian matrix has all positive eigenvalues, one can find stable structures of molecules (and ions). The Schrödinger equation is a necessary aspect of this process because the movement of the electrons is governed by this equation rather than by Newtonian classical equations. The information gained after carrying out such a geometry optimization process include (1) all of the inter-atomic distances and internal angles needed to specify the equilibrium geometry $\{R_{\text{aeq}}\}$ and (2) the total electronic energy E at this particular geometry.

It is also possible to extract much more information from these calculations. For example, by multiplying elements of the Hessian matrix $(\partial^2 E / \partial R_a \partial R_b)$ by the inverse square roots of the atomic masses of the atoms labeled a and b, one forms the mass-weighted Hessian $(m_a m_b)^{-1/2} (\partial^2 E / \partial R_a \partial R_b)$ whose non-zero eigenvalues give the harmonic vibrational frequencies $\{\omega_k\}$ of the molecule. The eigenvectors $\{R_{k,a}\}$ of the mass-weighted Hessian matrix give the relative displacements in coordinates $R_{k,a}$ that accompany vibration in the k^{th} normal mode (i.e., they describe the normal mode motions). Details about how these harmonic vibrational frequencies and normal modes are obtained were discussed earlier in Chapter 3.

5.1.2 Molecular Change- reactions and interactions

1. Changes in bonding

Chemistry also deals with transformations of matter including changes that occur when molecules react, are excited (electronically, vibrationally, or rotationally), or undergo geometrical rearrangements. Again, theory forms the cornerstone that allows experimental probes of chemical change to be connected to the molecular level and that allows simulations of such changes.

Molecular excitation may or may not involve altering the electronic structure of the molecule; vibrational and rotational excitation do not, but electronic excitation, ionization, and electron attachment do. As illustrated in Fig. 5.3 where a bi-molecular reaction is displayed, chemical reactions involve breaking some bonds and forming others, and thus involve rearrangement of the electrons among various molecular orbitals.

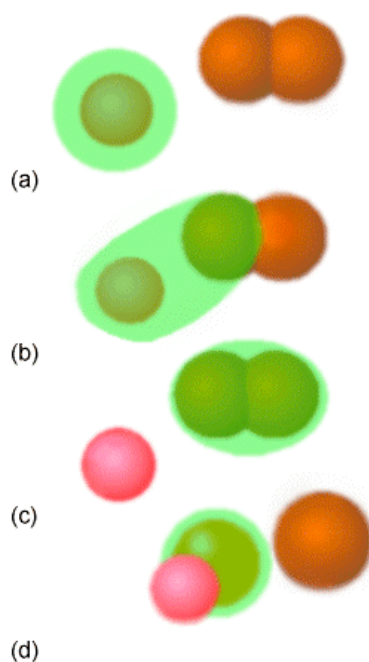


Figure 5.3 Two bimolecular reactions; a and b show an atom combining with a diatomic; c and d show an atom abstracting an atom from a diatomic.

In this example, in part (a) the green atom collides with the brown diatomic molecule and forms the bound triatomic molecule (b). Alternatively, in (c) and (d), a pink atom collides with a green diatomic to break the bond between the two green atoms and form a new bond between the pink and green atoms. Both such reactions are termed bi-molecular

because the basic step in which the reaction takes place requires a collision between two independent species (i.e., the atom and the diatomic).

A simple example of a unimolecular chemical reaction is offered by the arginine molecule considered above. In the first structure shown for arginine, the carboxylic acid group retains its HOOC- bonding. However, in the zwitterion structure of this same molecule, shown in Fig. 5.4, the HOOC- group has been deprotonated to produce a carboxylate anion group -COO^- , with the H^+ ion now bonded to the terminal imine group, thus converting it to an amino group and placing the net positive charge on the adjacent carbon atom. The unimolecular tautomerization reaction in which the two forms of arginine are interconverted involves breaking an O-H bond, forming a N-H bond, and changing a carbon-nitrogen double bond into a carbon-nitrogen single bond. In such a process, the electronic structure is significantly altered, and, as a result, the two isomers can display very different chemical reactivities toward other reagents. Notice that, once again, the ultimate structure of the zwitterion tautomer of arginine is determined by the valence preferences of its constituent atoms as well as by hydrogen bonds formed among various functional groups (the carboxylate group and one amino group and one -NH- group).

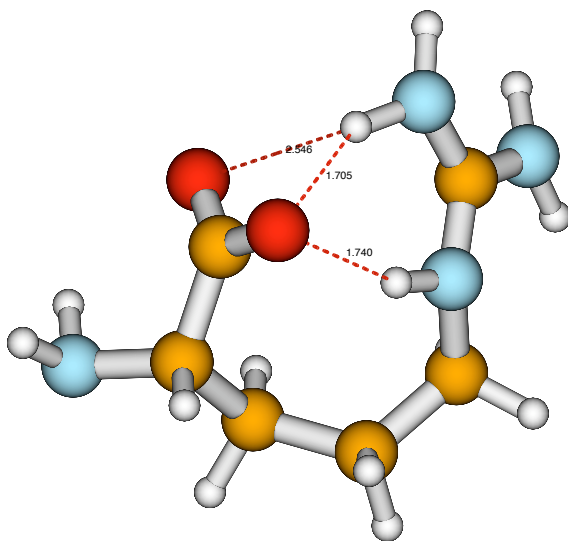


Figure 5.4 The arginine molecule in a zwitterion stable structure.

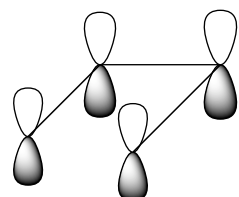
2. Energy Conservation

In any chemical reaction as in all physical processes (other than nuclear event in which mass and energy can be interconverted), total energy must be conserved. Reactions in which the summation of the strengths of all the chemical bonds in the reactants exceeds the sum of the bond strengths in the products are termed endothermic. For such reactions, external energy must be provided to the reacting molecules to allow the reaction to occur. Exothermic reactions are those for which the bonds in the products exceed in strength those of the reactants. For exothermic reactions, no net energy input is needed to allow the reaction to take place. Instead, excess energy is generated and liberated when such reactions take place. In the former (endothermic) case, the energy needed by the reaction usually comes from the kinetic energy of the reacting molecules or molecules that surround them. That is, thermal energy from the environment provides the needed energy. Analogously, for exothermic reactions, the excess energy produced as the reaction proceeds is usually deposited into the kinetic energy of the product molecules and into that of surrounding molecules. For reactions that are very endothermic, it may be virtually impossible for thermal excitation to provide sufficient energy to effect reaction. In such cases, it may be possible to use a light source (i.e., photons whose energy can excite the reactant molecules) to induce reaction. When the light source causes electronic excitation of the reactants (e.g., one might excite one electron in the bound diatomic molecule discussed above from a bonding to an anti-bonding orbital), one speaks of inducing reaction by photochemical means.

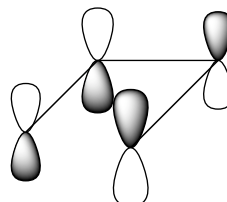
3. Conservation of Orbital Symmetry- the Woodward-Hoffmann Rules

An example of how important it is to understand the changes in bonding that accompany a chemical reaction, let us consider a reaction in which 1,3-butadiene is converted, via ring-closure, to form cyclobutene. Specifically, focus on the four π orbitals of 1,3-butadiene as the molecule undergoes so-called disrotatory closing along which the plane of symmetry which bisects and is perpendicular to the C_2-C_3 bond is preserved. The orbitals of the reactant and product can be labeled as being even-e or odd-o under reflection through this symmetry plane. It is not appropriate to label the orbitals with respect to their symmetry under the plane containing the four C atoms because, although

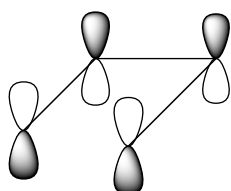
this plane is indeed a symmetry operation for the reactants and products, it does not remain a valid symmetry throughout the reaction path. That is, in applying the Woodward-Hoffmann rules, we symmetry label the orbitals using only those symmetry elements that are preserved throughout the reaction path being examined.



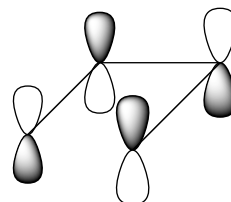
Lowest π orbital of
1,3- butadiene denoted
 π_1



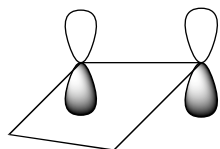
π_2



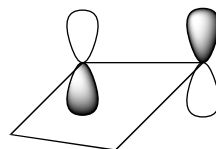
π_3



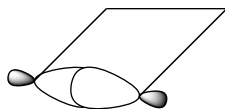
π_4



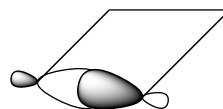
π orbital of
cyclobutene



π^* orbital of
cyclobutene



σ orbital of
cyclobutene



σ^* orbital of
cyclobutene

Figure 5.5 The active valence orbitals of 1, 3- butadiene and of cyclobutene.

The four π orbitals of 1,3-butadiene are of the following symmetries under the preserved symmetry plane (see the orbitals in Fig. 5.5): $\pi_1 = e$, $\pi_2 = o$, $\pi_3 = e$, $\pi_4 = o$. The π and π^* and σ and σ^* orbitals of the product cyclobutane, which evolve from the four orbitals of the 1,3-butadiene, are of the following symmetry and energy order: $\sigma = e$, $\pi = e$, $\pi^* = o$, $\sigma^* = o$. The Woodward-Hoffmann rules instruct us to arrange the reactant and product orbitals in order of increasing energy and to then connect these orbitals by symmetry, starting with the lowest energy orbital and going through the highest energy orbital. This process gives the following so-called orbital correlation diagram:

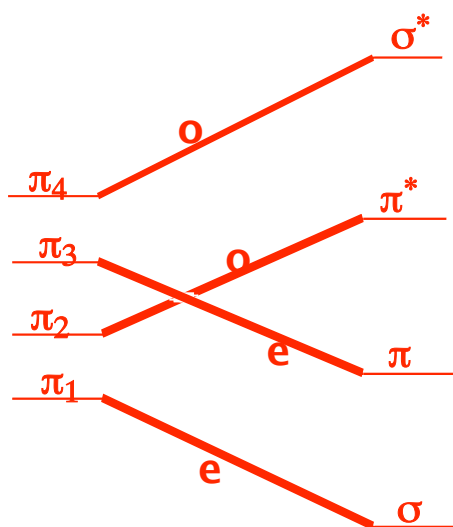


Figure 5.6 The orbital correlation diagram for the 1,3-butadiene to cyclobutene reaction.

We then need to consider how the electronic configurations in which the electrons are arranged as in the ground state of the reactants evolves as the reaction occurs.

We notice that the lowest two orbitals of the reactants, which are those occupied by the four π electrons of the reactant, do not connect to the lowest two orbitals of the products, which are the orbitals occupied by the two σ and two π electrons of the products. This causes the ground-state configuration of the reactants ($\pi_1^2 \pi_2^2$) to evolve into an excited configuration ($\sigma^2 \pi^{*2}$) of the products. This, in turn, produces an

activation barrier for the thermal disrotatory rearrangement (in which the four active electrons occupy these lowest two orbitals) of 1,3-butadiene to produce cyclobutene.

If the reactants could be prepared, for example by photolysis, in an excited state having orbital occupancy $\pi_1^2\pi_2^1\pi_3^1$, then reaction along the path considered would not have any symmetry-imposed barrier because this singly excited configuration correlates to a singly-excited configuration $\sigma^2\pi^1\pi^{*1}$ of the products. The fact that the reactant and product configurations are of equivalent excitation level causes there to be no symmetry constraints on the photochemically induced reaction of 1,3-butadiene to produce cyclobutene. In contrast, the thermal reaction considered first above has a symmetry-imposed barrier because the orbital occupancy is forced to rearrange (by the occupancy of two electrons from $\pi_2^2 = \pi^{*2}$ to $\pi^2 = \pi_3^2$) for the ground-state wave function of the reactant to smoothly evolve into that of the product. Of course, if the reactants could be generated in an excited state having $\pi_1^2\pi_3^2$ orbital occupancy, then products could also be produced directly in their ground electronic state. However, it is difficult, if not impossible, to generate such doubly-excited electronic states, so it is rare that one encounters reactions being induced via such states.

It should be stressed that although these symmetry considerations may allow one to anticipate barriers on reaction potential energy surfaces, they have nothing to do with the thermodynamic energy differences of such reactions. What the above Woodward-Hoffmann symmetry treatment addresses is whether there will be symmetry-imposed barriers above and beyond any thermodynamic energy differences. The enthalpies of formation of reactants and products contain the information about the reaction's overall energy balance and need to be considered independently of the kind of orbital symmetry analysis just introduced.

As the above example illustrates, whether a chemical reaction occurs on the ground or an excited-state electronic surface is important to be aware of. This example shows that one might want to photo-excite the reactant molecules to cause the reaction to occur at an accelerated rate. With the electrons occupying the lowest-energy orbitals, the ring closure reaction can still occur, but it has to surmount a barrier to do so (it can employ thermal collisional energy to surmount this barrier), so its rate might be slow. If an electron is excited, there is no symmetry barrier to surmount, so the rate can be

greater. Reactions that take place on excited states also have a chance to produce products in excited electronic states, and such excited-state products may emit light. Such reactions are called chemiluminescent because they produce light (luminescence) by way of a chemical reaction.

4. Rates of change

Rates of reactions play crucial roles in many aspects of our lives. Rates of various biological reactions determine how fast we metabolize food, and rates at which fuels burn in air determine whether an explosion or a calm flame will result. Chemists view the rate of any reaction among molecules (and perhaps photons or electrons if they are used to induce excitation in reactant molecules) to be related to (1) the frequency with which the reacting species encounter one another and (2) the probability that a set of such species will react once they do encounter one another. The former aspects relate primarily to the concentrations of the reacting species and the speeds with which they are moving. The latter have more to do with whether the encountering species collide in a favorable orientation (e.g., do the enzyme and substrate dock properly, or does the Br^- ion collide with the H_3C - end of $\text{H}_3\text{C-Cl}$ or with the Cl end in the $\text{S}_{\text{N}}2$ reaction that yields $\text{CH}_3\text{Br} + \text{Cl}^-$?) and with sufficient energy to surmount any barrier that must be passed to effect breaking bonds in reactants to form new bonds in products.

The rates of reactions can be altered by changing the concentrations of the reacting species, by changing the temperature, or by adding a catalyst. Concentrations and temperature control the collision rates among molecules, and temperature also controls the energy available to surmount barriers. Catalysts are molecules that are not consumed during the reaction but which cause the rate of the reaction to be increased (species that slow the rate of a reaction are called inhibitors). Most catalysts act by providing orbitals of their own that interact with the reacting molecules' orbitals to cause the energies of the latter to be lowered as the reaction proceeds. In the ring-closure reaction cited earlier, the catalyst's orbitals would interact (i.e., overlap) with the 1,3-butadiene's π orbitals in a manner that lowers their energies and thus reduces the energy barrier that must be overcome for reaction to proceed

In addition to being capable of determining the geometries (bond lengths and angles),

energies, vibrational frequencies of species such as the isomers of arginine discussed above, theory also addresses questions of how and how fast transitions among these isomers occur. The issue of how chemical reactions occur focuses on the mechanism of the reaction, meaning how the nuclei move and how the electronic orbital occupancies change as the system evolves from reactants to products. In a sense, understanding the mechanism of a reaction in detail amounts to having a mental moving picture of how the atoms and electrons move as the reaction is occurring.

The issue of how fast reactions occur relates to the rates of chemical reactions. In most cases, reaction rates are determined by the frequency with which the reacting molecules access a critical geometry (called the transition state or activated complex) near which bond breaking and bond forming takes place. The reacting molecules' potential energy along the path connecting reactants through a transition state to products is often represented as shown in Fig. 5.7.

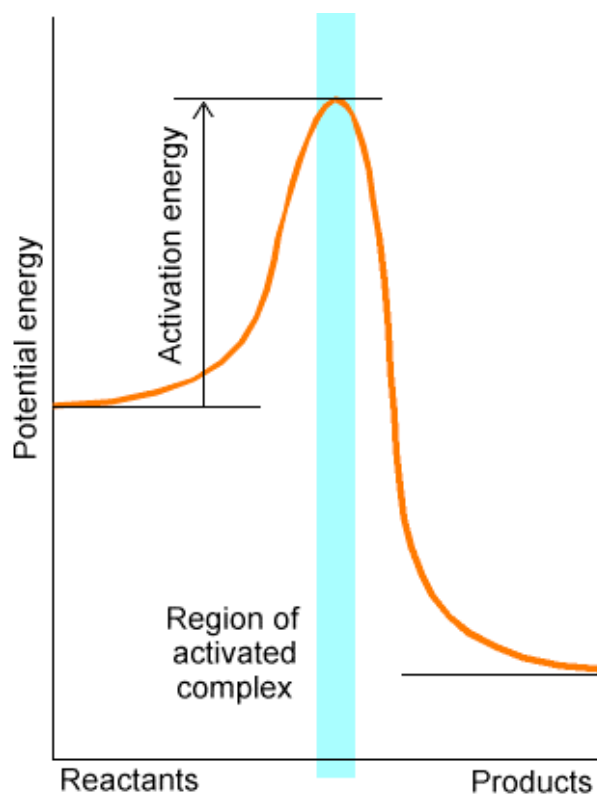


Figure 5.7 Energy vs. reaction progress plot showing the transition state or activated complex and the activation energy.

In this figure, the potential energy (i.e., the electronic energy without the nuclei's kinetic energy included) is plotted along a coordinate connecting reactants to products. The geometries and energies of the reactants, products, and of the activated complex can be determined using the potential energy surface searching methods discussed briefly above and detailed earlier in Chapter 3. Chapter 8 provides more information about the theory of reaction rates and how such rates depend upon geometrical, energetic, and vibrational properties of the reacting molecules.

The frequencies with which the transition state is accessed are determined by the amount of energy (termed the activation energy E^*) needed to access this critical geometry. For systems at or near thermal equilibrium, the probability of the molecule gaining energy E^* is shown for three temperatures in Fig. 5.8.

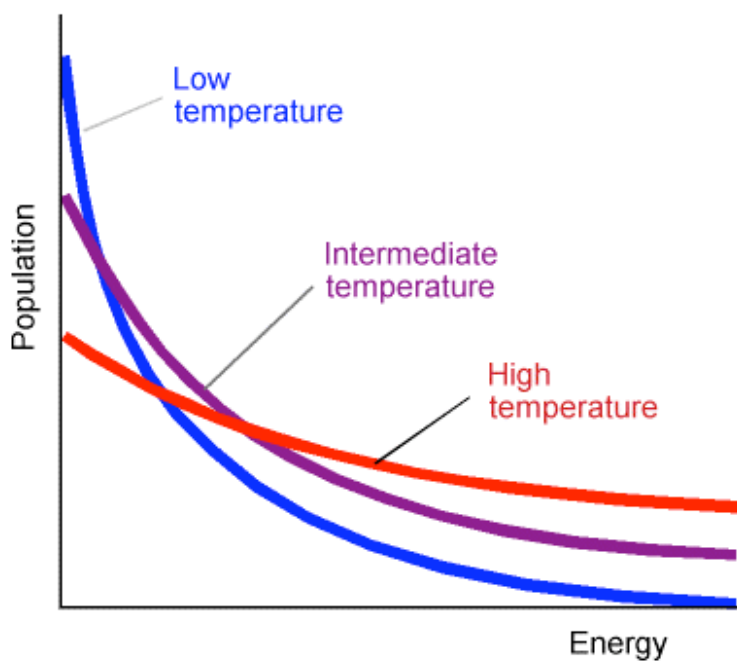


Figure 5.8 Distributions of energies at various temperatures.

For such cases, chemical reaction rates usually display a temperature dependence

characterized by linear plots of $\ln(k)$ vs $1/T$. Of course, not all reactions involve molecules that have been prepared at or near thermal equilibrium. For example, in supersonic molecular beam experiments, the kinetic energy distribution of the colliding molecules is more likely to be of the type shown in Fig. 5.9.

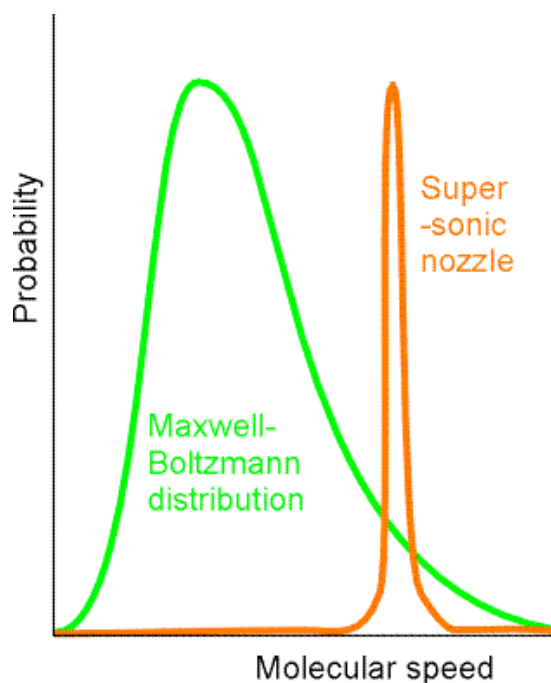


Figure 5.9 Molecular speed distributions in thermal and super-sonic beam cases.

In this figure, the probability is plotted as a function of the relative speed with which reactant molecules collide. It is common in making such collision speed plots to include the v^2 volume element factor in the plot. That is, the normalized probability distribution for molecules having reduced mass μ to collide with relative velocity components v_x, v_y, v_z is

$$P(v_x, v_y, v_z) dv_x dv_y dv_z = (\mu/2\pi kT)^{3/2} \exp(-\mu(v_x^2 + v_y^2 + v_z^2)/2kT) dv_x dv_y dv_z.$$

Because only the total collisional kinetic energy is important in surmounting reaction barriers, we convert this Cartesian velocity component distribution to one in terms of $v = (v_x^2 + v_y^2 + v_z^2)^{1/2}$ the collision speed. This is done by changing from Cartesian to polar coordinates (in which the radial variable is v itself) and gives (after integrating over the two angular coordinates):

$$P(v) dv = 4\pi (\mu/2\pi kT)^{3/2} \exp(-\mu v^2/2kT) v^2 dv.$$

It is the v^2 factor in this speed distribution that causes the Maxwell-Boltzmann distribution to vanish at low speeds in the above plot.

Another kind of experiment in which non-thermal conditions are used to extract information about activation energies occurs within the realm of ion-molecule reactions where one uses collision-induced dissociation (CID) to break a molecule apart. For example, when a complex consisting of a Na^+ cation bound to a uracil molecule is accelerated by an external electric field to a kinetic energy E and subsequently allowed to impact into a gaseous sample of Xe atoms, the high-energy collision allows kinetic energy to be converted into internal energy. This collisional energy transfer may deposit into the $\text{Na}^+(\text{uracil})$ complex enough energy to fragment the $\text{Na}^+ \dots \text{uracil}$ attractive binding energy, thus producing Na^+ and neutral uracil fragments. If the signal for production of Na^+ is monitored as the collision energy E is increased, one generates a CID reaction rate profile such as I show in Fig. 5.10.

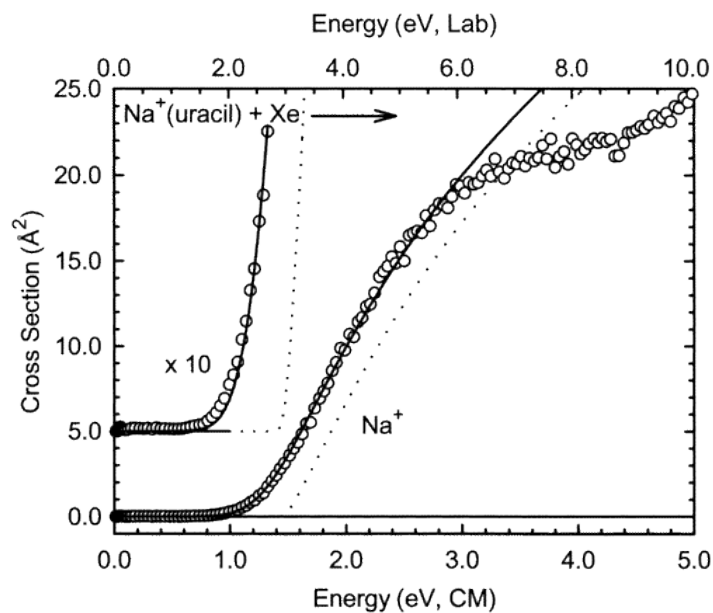


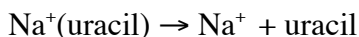
Figure 5.10 Reaction cross-section as a function of collision energy.

On the vertical axis is plotted a quantity proportional to the rate at which Na^+ ions are formed. On the horizontal axis is plotted the collision energy E in two formats. The laboratory kinetic energy is simply $1/2$ the mass of the $\text{Na}^+(\text{uracil})$ complex multiplied by the square of the speed of these ion complexes measured with respect to a laboratory-fixed coordinate frame. The center-of-mass (CM) kinetic energy is the amount of energy available between the $\text{Na}^+(\text{uracil})$ complex and the Xe atom, and is given by

$$E_{\text{CM}} = 1/2 m_{\text{complex}} m_{\text{Xe}} / (m_{\text{complex}} + m_{\text{Xe}}) v^2,$$

where v is the relative speed of the complex and the Xe atom, and m_{Xe} and m_{complex} are the respective masses of the colliding partners.

The most essential lesson to learn from such a graph is that no dissociation occurs if E is below some critical threshold value, and the CID reaction



occurs with higher and higher rate as the collision energy E increases beyond the threshold. For the example shown above, the threshold energy is ca. 1.2-1.4 eV. These CID thresholds can provide us with estimates of reaction endothermicities and are especially useful when these energies are greatly in excess of what can be realized by simply heating the sample.

5.1.3 Statistical Mechanics: Treating Large Numbers of Molecules in Close Contact

When one has a large number of molecules that undergo frequent collisions (thereby exchanging energy, momentum, and angular momentum), the behavior of this collection of molecules can often be described in a simple way. At first glance, it seems unlikely that the treatment of a large number of molecules could require far less effort than that required to describe one or a few such molecules.

To see the essence of what I am suggesting, consider a sample of 10 cm^3 of water at room temperature and atmospheric pressure. In this macroscopic sample, there are approximately 3.3×10^{23} water molecules. If one imagines having an instrument that could monitor the instantaneous speed of a selected molecule, one would expect the instrumental signal to display a very jerky irregular behavior if the signal were monitored on time scales of the order of the time between molecular collisions. On this time scale, the water molecule being monitored may be moving slowly at one instant, but, upon collision with a neighbor, may soon be moving very rapidly. In contrast, if one monitors the speed of this single water molecule over a very long time scale (i.e., much longer than the average time between collisions), one obtains an average square of the speed that is related to the temperature T of the sample via $1/2 mv^2 = 3/2 kT$. This relationship holds because the sample is at equilibrium at temperature T .

An example of the kind of behavior I describe above is shown in Fig. 5.11.

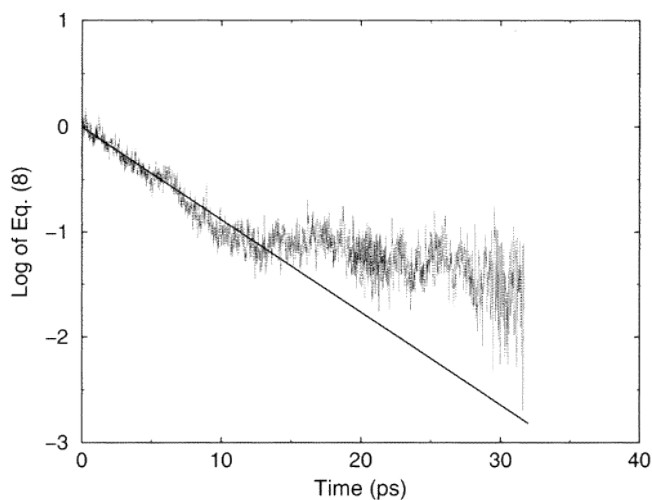


Figure 5.11 The energy possessed by a CN^- ion as a function of time.

In this figure, on the vertical axis is plotted the log of the energy (kinetic plus potential) of a single CN^- anion in a solution with water as the solvent as a function of time. The vertical axis label says Eq.(8) because this figure was taken from a literature article. The CN^- ion initially has excess vibrational energy in this simulation which was carried out in part to model the energy flow from this hot solute ion to the surrounding solvent molecules. One clearly sees the rapid jerks in energy that this ion experiences as it undergoes collisions with neighboring water molecules. These jerks occur approximately every 0.01 ps, and some of them correspond to collisions that take energy from the ion and others to collisions that given energy to the ion. On longer time scales (e.g., over 1-10 ps), we also see a gradual drop off in the energy content of the CN^- ion which illustrates the slow loss of its excess energy on the longer time scale.

Now, let's consider what happens if we monitor a large number of molecules rather than a single molecule within the 1 cm^3 sample of H_2O mentioned earlier. If we imagine drawing a sphere of radius R and monitoring the average speed of all water molecules within this sphere, we obtain a qualitatively different picture if the sphere is large enough to contain many water molecules. For large R , one finds that the average square of the speed of all the N water molecules residing inside the sphere (i.e., $\sum_{K=1,N} 1/2$

mv_k^2) is independent of time (even when considered at a sequence of times separated by fractions of ps) and is related to the temperature T through $\sum_k 1/2 mv_k^2 = 3N/2 kT$.

This example shows that, at equilibrium, the long-time average of a property of any single molecule is the same as the instantaneous average of this same property over a large number of molecules. For the single molecule, one achieves the average value of the property by averaging its behavior over time scales lasting for many, many collisions. For the collection of many molecules, the same average value is achieved (at any instant of time) because the number of molecules within the sphere (which is proportional to $4/3 \pi R^3$) is so much larger than the number near the surface of the sphere (proportional to $4\pi R^2$) that the molecules interior to the sphere are essentially at equilibrium for all times.

Another way to say the same thing is to note that the fluctuations in the energy content of a single molecule are very large (i.e., the molecule undergoes frequent large jerks) but last a short time (i.e., the time between collisions). In contrast, for a collection of many molecules, the fluctuations in the energy for the whole collection are small at all times because fluctuations take place by exchange of energy with the molecules that are not inside the sphere (and thus relate to the surface area to volume ratio of the sphere).

So, if one has a large number of molecules that one has reason to believe are at thermal equilibrium, one can avoid trying to follow the instantaneous short-time detailed dynamics of any one molecule or of all the molecules. Instead, one can focus on the average properties of the entire collection of molecules. What this means for a person interested in theoretical simulations of such condensed-media problems is that there is no need to carry out a Newtonian molecular dynamics simulation of the system (or a quantum simulation) if it is at equilibrium because the long-time averages of whatever is calculated can be found another way. How one achieves this is through the magic of statistical mechanics and statistical thermodynamics. One of the most powerful of the devices of statistical mechanics is the so-called Monte-Carlo simulation algorithm. Such theoretical tools provide a direct way to compute equilibrium averages (and small fluctuations about such averages) for systems containing large numbers of molecules. In Chapter 7, I provide a brief introduction to the basics of this sub-discipline of theoretical chemistry where you will learn more about this exciting field.

Sometimes we speak of the equilibrium behavior or the dynamical behavior of a collection of molecules. Let me elaborate a little on what these phrases mean. Equilibrium properties of molecular collections include the radial and angular distribution functions among various atomic centers. For example, the O-O and O-H radial distribution functions in liquid water and in ice are shown in Fig. 5.12.

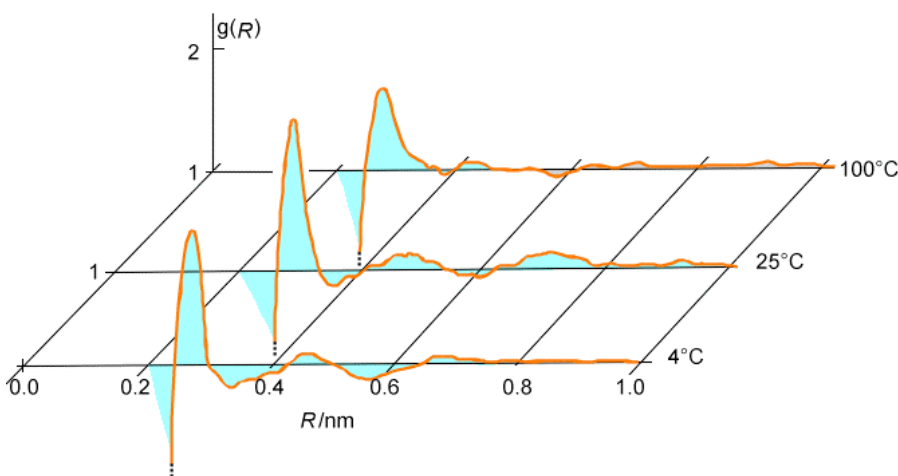


Figure 5.12 Radial O-O distribution functions at three temperatures.

Such properties represent averages, over long times or over a large collection of molecules, of some property that is not changing with time except on a very fast time scale corresponding to individual collisions.

In contrast, dynamical properties of molecular collections include the folding and unfolding processes that proteins and other polymers undergo; the migrations of protons from water molecule to water molecule in liquid water and along H₂O chains within ion channels; and the self assembly of molecular monolayers on solid surfaces as the concentration of the molecules in the liquid overlayer varies. These are properties that occur on time scales much longer than those between molecular collisions and on time scales that we wish to probe by some experiment or by simulation.

Having briefly introduced the primary areas of theoretical chemistry- structure, dynamics, and statistical mechanics, let us now examine each of them in somewhat greater detail, keeping in mind that Chapters 6-8 are where each is treated more fully.

5.2 Molecular Structure: Theory and Experiment

5.2.1 Experimental Probes of Molecular Shapes

I expect you are wondering why I want to discuss how experiments measure molecular shapes in this text whose aim is to introduce you to the field of theoretical chemistry. In fact, theory and experimental measurement are very connected, and it is these connections that I wish to emphasize in the following discussion. In particular, I want to make it clear that experimental data can only be interpreted, and thus used to extract molecular properties, through the application of theory. So, theory does not replace experiment, but serves both as a complementary component of chemical research (via. simulation of molecular properties) and as the means by which we connect laboratory data to molecular properties.

1. Rotational Spectroscopy

Most of us use rotational excitation of molecules in our every-day life. In particular, when we cook in a microwave oven, the microwave radiation, which has a frequency in the 10^9 - 10^{11} s^{-1} range, inputs energy into the rotational motions of the (primarily) water molecules contained in the food. These rotationally hot water molecules then collide with neighboring molecules (i.e., other water as well as proteins and other molecules in the food and in the cooking vessel) to transfer some of their motional energy to them. Through this means, the translational kinetic energy of all the molecules inside the cooker gains energy. This process of rotation-to-translation energy transfer is how the microwave radiation ultimately heats the food, which cooks it. What happens when you put the food into the microwave oven in a metal container or with some other metal material? As shown in Chapter 2, the electrons in metals exist in very delocalized partially filled orbitals called bands. These band orbitals are spread out throughout the entire piece of metal. The application of any external electric field (e.g., that belonging to the microwave radiation) causes these metal electrons to move throughout the metal. As these electrons accumulate more and more energy from the microwave radiation, they eventually have enough kinetic energy to be ejected into the surrounding air forming a discharge. This causes the sparking that we see when we make the mistake of putting

anything metal into our microwave oven. Let's now learn more about how the microwave photons cause the molecules to become rotationally excited.

Using microwave radiation, molecules having dipole moment vectors (μ) can be made to undergo rotational excitation. In such processes, the time-varying electric field $E \cos(\omega t)$ of the microwave electromagnetic radiation interacts with the molecules via a potential energy of the form $V = \mathbf{E} \cdot \mu \cos(\omega t)$. This potential can cause energy to flow from the microwave energy source into the molecule's rotational motions when the energy of the former $h\omega/2\pi$ matches the energy spacing between two rotational energy levels.

This idea of matching the energy of the photons to the energy spacings of the molecule illustrates the concept of resonance and is something that is ubiquitous in spectroscopy as we learned in mathematical detail in Chapter 4. Upon first hearing that the photon's energy must match an energy-level spacing in the molecule if photon absorption is to occur, it appears obvious and even trivial. However, upon further reflection, there is more to such resonance requirements than one might think. Allow me to illustrate using this microwave-induced rotational excitation example by asking you to consider why photons whose energies $h\omega/2\pi$ considerably exceed the energy spacing ΔE will not be absorbed in this transition. That is, why is more than enough energy not good enough? The reason is that for two systems (in this case the photon's electric field and the molecule's rotation which causes its dipole moment to also rotate) to interact and thus exchange energy (this is what photon absorption is), they must have very nearly the same frequencies. If the photon's frequency (ω) exceeds the rotational frequency of the molecule by a significant amount, the molecule will experience an electric field that oscillates too quickly to induce a torque on the molecule's dipole that is always in the same direction and that lasts over a significant length of time. As a result, the rapidly oscillating electric field will not provide a coherent twisting of the dipole and hence will not induce rotational excitation.

One simple example from every day life can further illustrate this issue. When you try to push your friend, spouse, or child on a swing, you move your arms in resonance with the swinging person's movement frequency. Each time the person returns to you, your arms are waiting to give a push in the direction that gives energy to the

swinging individual. This happens over and over again; each time they return, your arms have returned to be ready to give another push in the same direction. In this case, we say that your arms move in resonance with the swing's motion and offer a coherent excitation of the swinger. If you were to increase greatly the rate at which your arms are moving in their up and down pattern, the swinging person would not always experience a push in the correct direction when they return to meet your arms. Sometimes they would feel a strong in-phase push, but other times they would feel an out-of-phase push in the opposite direction. The net result is that, over a long period of time, they would feel random jerks from your arms, and thus would not undergo smooth energy transfer from you. This is why too high a frequency (and hence too high an energy) does not induce excitation. Let us now return to the case of rotational excitation by microwave photons.

As we saw in Chapter 2, for a rigid diatomic molecule, the rotational energy spacings are given by

$$E_{J+1} - E_J = 2(J+1) (\hbar^2/2I) = 2hc B (J+1),$$

where I is the moment of inertia of the molecule given in terms of its equilibrium bond length r_e and its reduced mass $\mu = m_a m_b / (m_a + m_b)$ as $I = \mu r_e^2$. Thus, in principle, measuring the rotational energy level spacings via microwave spectroscopy allows one to determine r_e . The second identity above simply defines what is called the rotational constant B in terms of the moment of inertia. The rotational energy levels described above give rise to a manifold of levels of non-uniform spacing as shown in the Fig. 5.13.

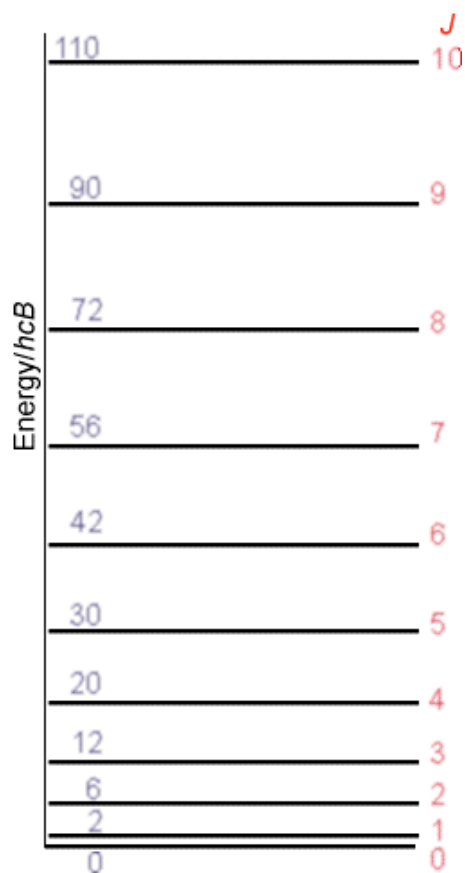


Figure 5.13 Rotational energy levels vs. rotational quantum number.

The non-uniformity in spacings is a result of the quadratic dependence of the rotational energy levels E_J on the rotational quantum number J :

$$E_J = J(J+1) (\hbar^2 / 2I).$$

Moreover, the level with quantum number J is $(2J+1)$ -fold degenerate; that is, there are $2J+1$ distinct energy states and wave functions that have energy E_J and that are distinguished by a quantum number M . These $2J+1$ states have identical energy but differ among one another by the orientation of their angular momentum in space (i.e., the orientation of how they are spinning).

For polyatomic molecules, we know from Chapter 2 that things are more complicated because the rotational energy levels depend on three so-called principal

moments of inertia (I_a , I_b , I_c) which, in turn, contain information about the molecule's geometry. These three principle moments are found by forming a 3x3 moment of inertia matrix having elements

$$I_{x,x} = \sum_a m_a [(R_a - R_{\text{CofM}})^2 - (x_a - x_{\text{CofM}})^2]; \text{ and } I_{x,y} = \sum_a m_a [(x_a - x_{\text{CofM}}) (y_a - y_{\text{CofM}})]$$

expressed in terms of the Cartesian coordinates of the nuclei (a) and of the center of mass in an arbitrary molecule-fixed coordinate system (analogous definitions hold for $I_{z,z}$, $I_{y,y}$, $I_{x,z}$ and $I_{y,z}$). The principle moments are then obtained as the eigenvalues of this 3x3 matrix.

For molecules with all three principle moments equal, the rotational energy levels are given by $E_{J,K} = \hbar^2 J(J+1)/2I$, and are independent of the K quantum number and on the M quantum number that again describes the orientation of how the molecule is spinning in space. Such molecules are called spherical tops. For molecules (called symmetric tops) with two principle moments equal (I_a) and one unique moment I_c , the energies depend on two quantum numbers J and K and are given by $E_{J,K} = \hbar^2 J(J+1)/2I_a + \hbar^2 K^2 (1/2I_c - 1/2I_a)$. Species having all three principal moments of inertia unique, termed asymmetric tops, have rotational energy levels for which no analytic formula is yet known. The H_2O molecule, shown in Fig. 5.14, is such an asymmetric top molecule. More details about the rotational energies and wave functions were given in Chapter 2.

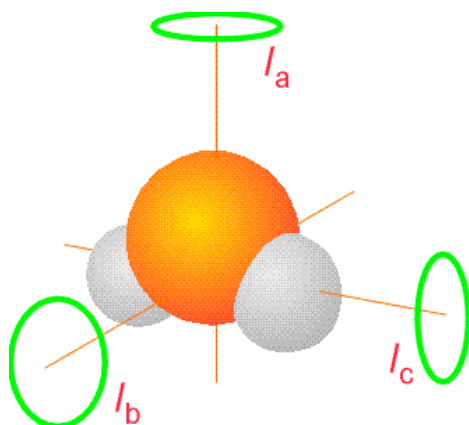


Figure 5.14 Water molecule showing its three distinct principal moment of inertia.

The moments of inertia that occur in the expressions for the rotational energy levels involve positions of atomic nuclei relative to the center of mass of the molecule. So, a microwave spectrum can, in principle, determine the moments of inertia and hence the geometry of a molecule. In the discussion given above, we treated these positions, and thus the moments of inertia as fixed (i.e., not varying with time). Of course, these distances are not unchanging with time in a real molecule because the molecule's atomic nuclei undergo vibrational motions. Because of this, it is the vibrationally-averaged moments of inertia that must be incorporated into the rotational energy level formulas. Specifically, because the rotationally energies depend on the inverses of moments of inertia, one must vibrationally average $(R_a - R_{\text{CoM}})^{-2}$ over the vibrational motion that characterizes the molecule's movement. For species containing stiff bonds, the vibrational average $\langle v | (R_a - R_{\text{CoM}})^{-2} | v \rangle$ of the inverse squares of atomic distances relative to the center of mass does not differ significantly from the equilibrium values $(R_{a,\text{eq}} - R_{\text{CoM}})^{-2}$ of the same distances. However, for molecules such as weak van der Waals complexes (e.g., $(\text{H}_2\text{O})_2$ or $\text{Ar} \cdot \text{HCl}$) that undergo floppy large-amplitude vibrational motions, there may be large differences between the equilibrium $(R_{a,\text{eq}} - R_{\text{CoM}})^{-2}$ and the vibrationally averaged values $\langle v | (R_a - R_{\text{CoM}})^{-2} | v \rangle$. The proper treatment of the rotational energy level patterns in such floppy molecules is still very much under active study by theoretical and experimental chemists. For this reason, it is a very challenging task to use microwave data on rotational energies to determine geometries (equilibrium or vibrationally averaged) for these kinds of molecules.

So, in the area of rotational spectroscopy theory plays several important roles:

- a. It provides the basic equations in terms of which the rotational line spacings relate to moments of inertia.
- b. It allows one, given the distribution of geometrical bond lengths and angles characteristic of the vibrational state the molecule exists in, to compute the proper vibrationally-averaged moment of inertia.
- c. It can be used to treat large amplitude floppy motions (e.g., by simulating the nuclear motions on a Born-Oppenheimer energy surface), thereby allowing rotationally resolved spectra of such species to provide proper moment of inertia (and thus geometry) information.

2. Vibrational Spectroscopy

The ability of molecules to absorb and emit infrared radiation as they undergo transitions among their vibrational energy levels is critical to our planet's health. It turns out that water and CO₂ molecules have bonds that vibrate in the 10^{13} - 10^{14} s⁻¹ frequency range which is within the infrared spectrum (10^{11} – 10^{14} s⁻¹). As solar radiation (primarily visible and ultraviolet) impacts the earth's surface, it is absorbed by molecules with electronic transitions in this energy range (e.g., colored molecules such as those contained in plant leaves and other dark material). These molecules are thereby promoted to excited electronic states. Some such molecules re-emit the photons that excited them but most undergo so-called radiationless relaxation that allows them to return to their ground electronic state but with a substantial amount of internal vibrational energy. That is, these molecules become vibrationally very hot. Subsequently, these hot molecules, as they undergo transitions from high-energy vibrational levels to lower-energy levels, emit infrared (IR) photons.

If our atmosphere were devoid of water vapor and CO₂, these IR photons would travel through the atmosphere and be lost into space. The result would be that much of the energy provided by the sun's visible and ultraviolet photons would be lost via IR emission. However, the water vapor and CO₂ do not allow so much IR radiation to escape. These greenhouse gases absorb the emitted IR photons to generate vibrationally hot water and CO₂ molecules in the atmosphere. These vibrationally excited molecules undergo collisions with other molecules in the atmosphere and at the earth's surface. In such collisions, some of their vibrational energy can be transferred to translational kinetic energy of the collision-partner molecules. In this manner, the temperature (which is a measure of the average translational energy) increases. Of course, the vibrationally hot molecules can also re-emit their IR photons, but there is a thick layer of such molecules forming a blanket around the earth, and all of these molecules are available to continually absorb and re-emit the IR energy. In this manner, the blanket keeps the IR radiation from escaping and thus keeps our atmosphere warm. Those of us who live in dry desert climates are keenly aware of such effects. Clear cloudless nights in the desert can become very cold, primarily because much of the day's IR energy production is lost to radiative

emission through the atmosphere and into space. Let's now learn more about molecular vibrations, how IR radiation excites them, and what theory has to do with this.

When infrared (IR) radiation is used to excite a molecule, it is the vibrations of the molecule that are in resonance with the oscillating electric field $\mathbf{E} \cos(\omega t)$. Molecules that have dipole moments that vary as its vibrations occur interact with the IR electric field via a potential energy of the form $V = (\partial\boldsymbol{\mu}/\partial Q) \cdot \mathbf{E} \cos(\omega t)$. Here $\partial\boldsymbol{\mu}/\partial Q$ denotes the change in the molecule's dipole moment $\boldsymbol{\mu}$ associated with motion along the vibrational normal mode labeled Q .

As the IR radiation is scanned, it comes into resonance with various vibrations of the molecule under study, and radiation can be absorbed. Knowing the frequencies at which radiation is absorbed provides knowledge of the vibrational energy level spacings in the molecule. Absorptions associated with transitions from the lowest vibrational level to the first excited level are called fundamental transitions. Those connecting the lowest level to the second excited state are called first overtone transitions. Excitations from excited levels to even higher levels are named hot-band absorptions.

Fundamental vibrational transitions occur at frequencies that characterize various functional groups in molecules (e.g., O-H stretching, H-N-H bending, N-H stretching, C-C stretching, etc.). As such, a vibrational spectrum offers an important fingerprint that allows the chemist to infer which functional groups are present in the molecule. However, when the molecule contains soft floppy vibrational modes, it is often more difficult to use information about the absorption frequency to extract quantitative information about the molecule's energy surface and its bonding structure. As was the case for rotational levels of such floppy molecules, the accurate treatment of large-amplitude vibrational motions of such species remains an area of intense research interest within the theory community.

In a polyatomic molecule with N atoms, there are many vibrational modes. The total vibrational energy of such a molecule can be approximated as a sum of terms, one for each of the $3N-6$ (or $3N-5$ for a linear molecule) vibrations:

$$E(v_1 \cdots v_{3N-5 \text{ or } 6}) = \sum_{j=1}^{3N-5 \text{ or } 6} \hbar\omega_j (v_j + 1/2).$$

Here, ω_j is the harmonic frequency of the j^{th} mode and v_j is the vibrational quantum number associated with that mode. As we discussed in Chapter 3, the vibrational wave functions are products of harmonic vibrational functions for each mode:

$$\psi = \prod_{j=1,3,5 \text{ or } 6} \psi_{v_j}(x^{(j)}),$$

and the spacings between energy levels in which one of the normal-mode quantum numbers increases by unity are expressed as

$$\Delta E_{v_j} = E(\dots v_j + 1 \dots) - E(\dots v_j \dots) = \hbar \omega_j.$$

That is, the spacings between successive vibrational levels of a given mode are predicted to be independent of the quantum number v within this harmonic model as shown in Fig. 5.15.

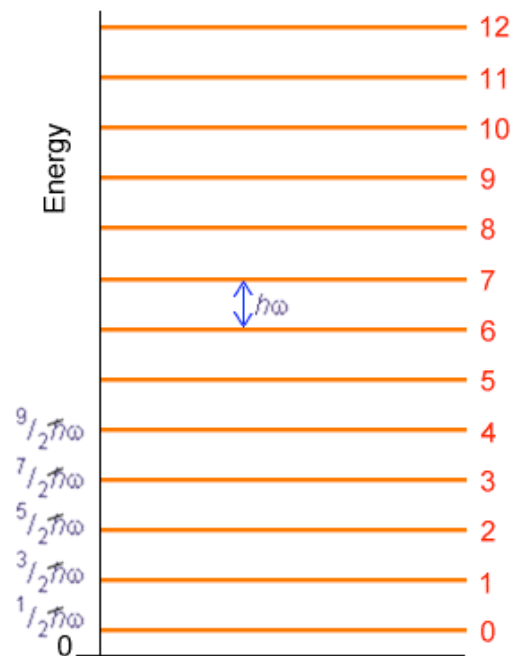


Figure 5.15 Harmonic vibrational energy levels vs. vibrational quantum number.

In Chapter 3, the details connecting the local curvature (i.e., Hessian matrix elements) in a polyatomic molecule's potential energy surface to its normal modes of vibration are presented.

Experimental evidence clearly indicates that significant deviations from the harmonic oscillator energy expression occur as the quantum number v_j grows. These deviations are explained in terms of the molecule's true potential $V(R)$ deviating strongly from the harmonic $1/2k (R-R_e)^2$ potential at higher energy as shown in the Fig. 5.16.

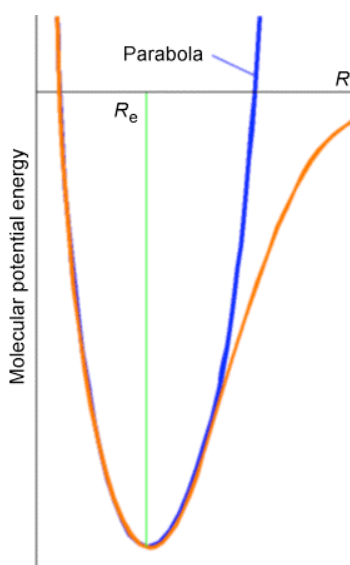


Figure 5.16 Harmonic (parabola) and anharmonic potentials.

At larger bond lengths, the true potential is softer than the harmonic potential, and eventually reaches its asymptote, which lies at the dissociation energy D_e above its minimum. This deviation of the true $V(R)$ from $1/2 k(R-R_e)^2$ causes the true vibrational energy levels to lie below the harmonic predictions.

It is convention to express the experimentally observed vibrational energy levels, along each of the $3N-5$ or 6 independent modes in terms of an anharmonic formula similar to what we discussed for the Morse potential in Chapter 2:

$$E(v_j) = \hbar[\omega_j (v_j + 1/2) - (\omega x)_j (v_j + 1/2)^2 + (\omega y)_j (v_j + 1/2)^3 + (\omega z)_j (v_j + 1/2)^4 + \dots]$$

The first term is the harmonic expression. The next is termed the first anharmonicity; it (usually) produces a negative contribution to $E(v_j)$ that varies as $(v_j + 1/2)^2$. Subsequent terms are called higher anharmonicity corrections. The spacings between successive $v_j \rightarrow v_j + 1$ energy levels are then given by:

$$\begin{aligned} \Delta E_{v_j} &= E(v_j + 1) - E(v_j) \\ &= \hbar [\omega_j - 2(\omega x)_j (v_j + 1) + \dots] \end{aligned}$$

A plot of the spacing between neighboring energy levels versus v_j should be linear for values of v_j where the harmonic and first anharmonicity terms dominate. The slope of such a plot is expected to be $-2\hbar(\omega x)_j$ and the small $-v_j$ intercept should be $\hbar[\omega_j - 2(\omega x)_j]$. Such a plot of experimental data, which clearly can be used to determine the ω_j and $(\omega x)_j$ parameters of the vibrational mode of study, is shown in Fig. 5.17.

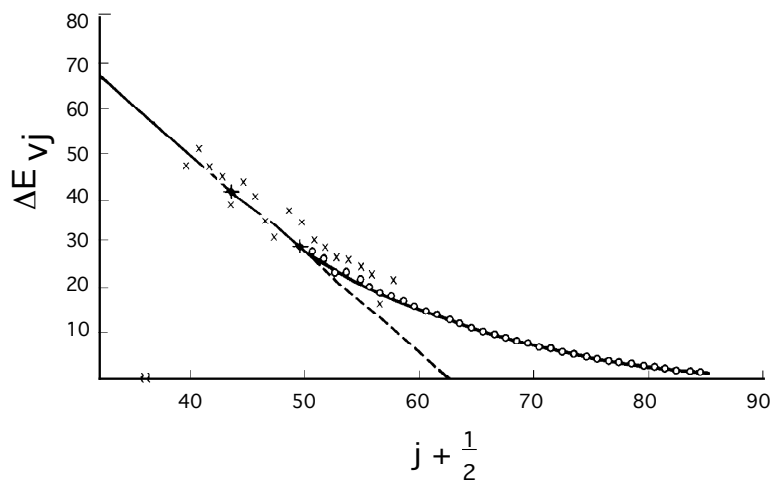


Figure 5.17 Birge-Sponer plot of vibrational energy spacings vs. quantum number.

These so-called Birge-Sponer plots can also be used to determine dissociation energies of molecules if the vibration whose spacings are plotted corresponds to a bond-stretching mode. By linearly extrapolating such a plot of experimental ΔE_{v_j} values to large v_j values, one can find the value of v_j at which the spacing between neighboring vibrational levels goes to zero. This value $v_{j, \max}$ specifies the quantum number of the last bound vibrational level for the particular bond-stretching mode of interest. The dissociation energy D_e can then be computed by adding to $1/2\hbar\omega_j$ (the zero point energy along this mode) the sum of the spacings between neighboring vibrational energy levels from $v_j = 0$ to $v_j = v_{j, \max}$:

$$D_e = 1/2\hbar\omega_j + \sum_{v_j=0}^{v_{j, \max}} \Delta E_{v_j}.$$

So, in the case of vibrational spectroscopy, theory allows us to

- i. interpret observed infrared lines in terms of absorptions arising in localized functional groups;
- ii. extract dissociation energies if a long progression of lines is observed in a bond-stretching transition;
- iii. and treat highly non-harmonic floppy vibrations by carrying out dynamical simulations on a Born-Oppenheimer energy surface.

3. X-Ray Crystallography

In x-ray crystallography experiments, one employs crystalline samples of the molecules of interest and makes use of the diffraction patterns produced by scattered x-rays to determine positions of the atoms in the molecule relative to one another using the famous Bragg formula:

$$n\lambda = 2d \sin\theta.$$

In this equation, λ is the wavelength of the x-rays, d is a spacing between layers (planes) of atoms in the crystal, θ is the angle through which the x-ray beam is scattered, and n is an integer (1,2, ...) that labels the order of the scattered beam.

Because the x-rays scatter most strongly from the inner-shell electrons of each atom, the interatomic distances obtained from such diffraction experiments are, more precisely, measures of distances between high electron densities in the neighborhoods of various atoms. The x-rays interact most strongly with the inner-shell electrons because it is these electrons whose characteristic Bohr frequencies of motion are (nearly) in resonance with the high frequency of such radiation. For this reason, x-rays can be viewed as being scattered from the core electrons that reside near the nuclear centers within a molecule. Hence, x-ray diffraction data offers a very precise and reliable way to probe inter-atomic distances in molecules.

The primary difficulties with x-ray measurements are:

- i. That one needs to have crystalline samples (often, materials simply cannot be grown as crystals),
- ii. That one learns about inter-atomic spacings as they occur in the crystalline state, not as they exist, for example, in solution or in gas-phase samples. This is especially problematic for biological systems where one would like to know the

structure of the bio-molecule as it exists within the living organism.

Nevertheless, x-ray diffraction data and its interpretation through the Bragg formula provide one of the most widely used and reliable ways for probing molecular structure.

4. NMR Spectroscopy

NMR spectroscopy probes the absorption of radio-frequency (RF) radiation by the nuclear spins of the molecule. The most commonly occurring spins in natural samples are ^1H (protons), ^2H (deuterons), ^{13}C and ^{15}N nuclei. In the presence of an external magnetic field $B_0\mathbf{z}$ along the z-axis, each such nucleus has its spin states split in energy by an amount given by $B_0(1-\sigma_k)\gamma_k M_I$, where M_I is the component of the k^{th} nucleus' spin angular momentum along the z-axis, B_0 is the strength of the external magnetic field, and γ_k is a so-called gyromagnetic factor (i.e., a constant) that is characteristic of the k^{th} nucleus. This splitting of magnetic spin levels by a magnetic field is called the Zeeman effect, and it is illustrated in Fig. 5.18.

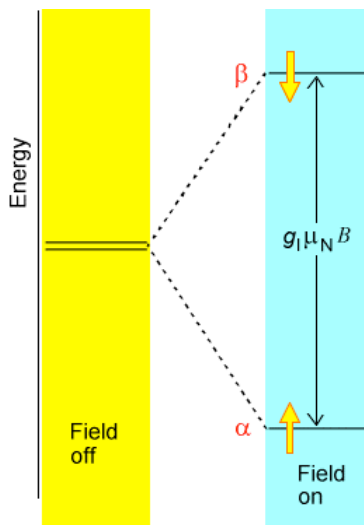


Figure 5.18 Zeeman splitting of magnetic nucleus's two levels caused by magnetic field.

The factor $(1-\sigma_k)$ is introduced to describe the screening of the external B_0 -field at the k^{th} nucleus caused by the electron cloud that surrounds this nucleus. In effect, $B_0(1-\sigma_k)$ is the

magnetic field experienced local to the k^{th} nucleus. It is this $(1-\sigma_k)$ screening that gives rise to the phenomenon of chemical shifts in NMR spectroscopy, and it is this factor that allows NMR measurements of shielding factors (σ_k) to be related, by theory, to the electronic environment of a nucleus. In Fig. 5.19 we display the chemical shifts of proton and ^{13}C nuclei in a variety of chemical bonding environments.

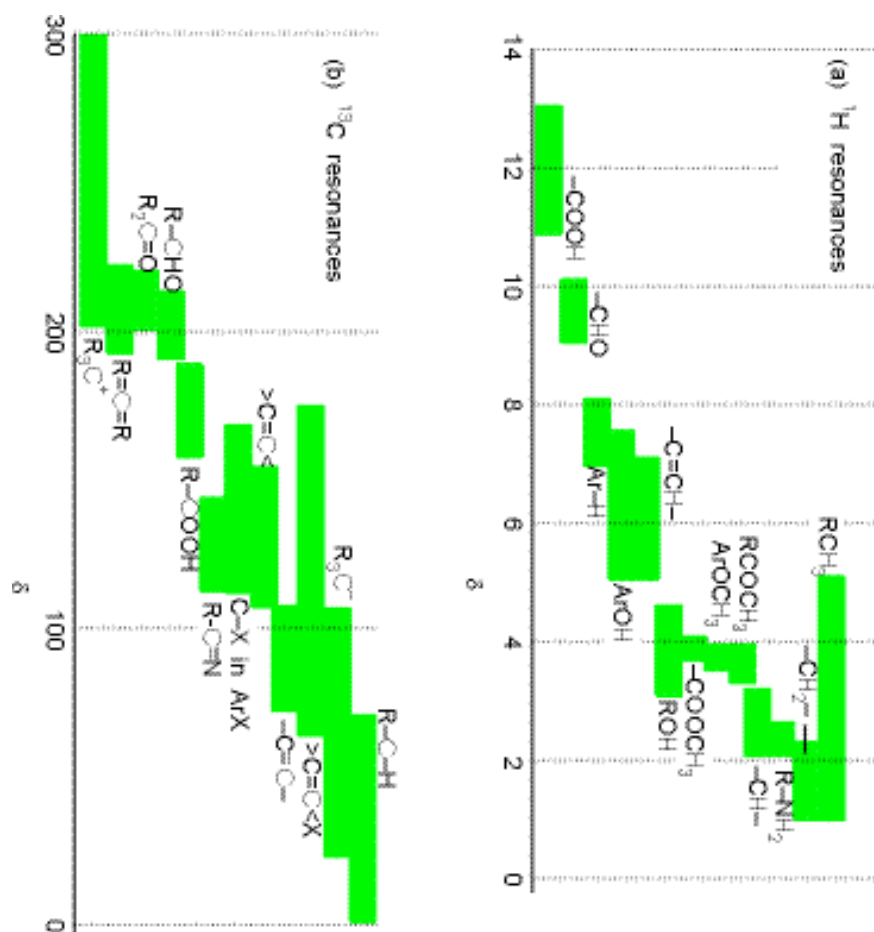


Figure 5.19 Chemical shifts characterizing various electronic environments for protons and for carbon-13 nuclei.

Because the M_l quantum number changes in steps of unity and because each photon possesses one unit of angular momentum, the RF energy $\hbar\omega$ that will be in resonance with the k^{th} nucleus' Zeeman-split levels is given by $\hbar\omega = B_0(1-\sigma_k)\gamma_k$.

In most NMR experiments, a fixed RF frequency is employed and the external magnetic field is scanned until the above resonance condition is met. Determining at what B_0 value a given nucleus absorbs RF radiation allows one to determine the local shielding ($1-\sigma_k$) for that nucleus. This, in turn, provides information about the electronic environment local to that nucleus as illustrated in the above figure. This data tells the chemist a great deal about the molecule's structure because it suggests what kinds of functional groups occur within the molecule.

To extract even more geometrical information from NMR experiments, one makes use of another feature of nuclear spin states. In particular, it is known that the energy levels of a given nucleus (e.g., the k^{th} one) are altered by the presence of other nearby nuclear spins. These spin-spin coupling interactions give rise to splittings in the energy levels of the k^{th} nucleus that alter the above energy expression as follows:

$$E_M = B_0(1-\sigma_k)\gamma_k M + J M M'$$

Where M is the z -component of the k^{th} nuclear spin angular momentum, M' is the corresponding component of a nearby nucleus causing the splitting, and J is called the spin-spin coupling constant between the two nuclei.

Examples of how spins on neighboring centers split the NMR absorption lines of a given nucleus are shown in Figs. 5.20-5.22 for three common cases. The first involves a nucleus (labeled A) that is close enough to one other magnetically active nucleus (labeled X); the second involves a nucleus (A) that is close to two equivalent nuclei (2X); and the third describes a nucleus (A) close to three equivalent nuclei (X3).

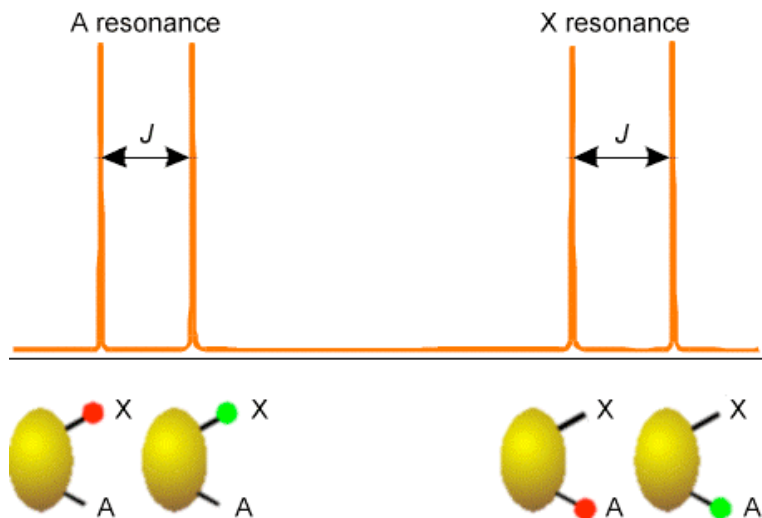


Figure 5.20 Splitting pattern characteristic of AX case

In Fig. 5.20 are illustrated the splitting in the X nucleus' absorption due to the presence of a single A neighbor nucleus (right) and the splitting in the A nucleus' absorption (left) caused by the X nucleus. In both of these examples, the X and A nuclei have only two M_I values, so they must be spin-1/2 nuclei. This kind of splitting pattern would, for example, arise for a ^{13}C -H group in the benzene molecule where $A = ^{13}\text{C}$ and $X = ^1\text{H}$.

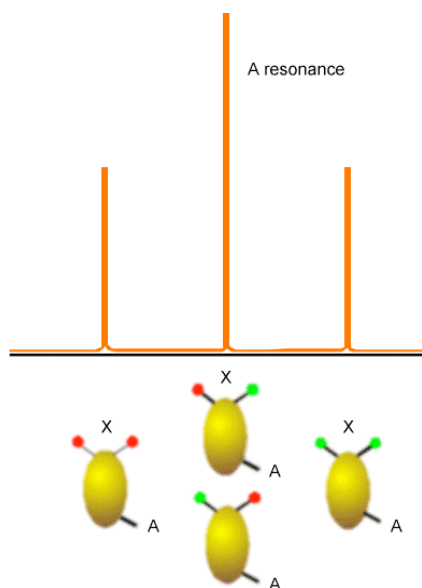


Figure 5.21 Splitting pattern characteristic of AX2 case

The (AX₂) splitting pattern shown in Fig. 5.21 would, for example, arise in the ¹³C spectrum of a –CH₂– group, and illustrates the splitting of the A nucleus' absorption line by the four spin states that the two equivalent X spins can occupy. Again, the lines shown would be consistent with X and A both having spin 1/2 because they each assume only two M_I values.

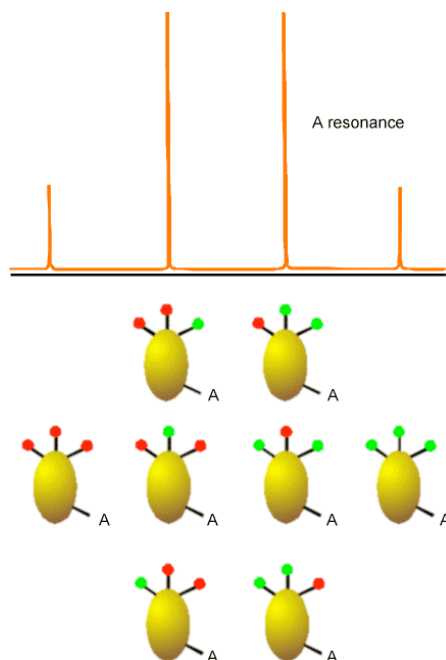


Figure 5.22 Splitting pattern characteristic of AX₃ case

In Fig. 5.22 is the kind of splitting pattern (AX₃) that would apply to the ¹³C NMR absorptions for a –CH₃ group. In this case, the spin-1/2 A line is split by the eight spin states that the three equivalent spin-1/2 H nuclei can occupy.

The magnitudes of these J coupling constants depend on the distances R between the two nuclei to the inverse sixth power (i.e., as R⁻⁶). They also depend on the γ values of the two interacting nuclei. In the presence of splitting caused by nearby (usually covalently bonded) nuclei, the NMR spectrum of a molecule consists of sets of absorptions (each belonging to a specific nuclear type in a particular chemical environment and thus have a specific chemical shift) that are split by their couplings to the other nuclei. Because of the spin-spin coupling's strong decay with internuclear distance, the magnitude and

pattern of the splitting induced on one nucleus by its neighbors provides a clear signature of what the neighboring nuclei are (i.e., through the number of M' values associated with the peak pattern) and how far these nuclei are (through the magnitude of the J constant, knowing it is proportional to R^{-6}). This near-neighbor data, combined with the chemical shift functional group data, offer powerful information about molecular structure.

An example of a full NMR spectrum is given in Fig. 5.23 where the ^1H spectrum (i.e., only the proton absorptions are shown) of $\text{H}_3\text{C}-\text{H}_2\text{C}-\text{OH}$ appears along with plots of the integrated intensities under each set of peaks. The latter data suggests the total number of nuclei corresponding to that group of peaks. Notice how the OH proton's absorption, the absorption of the two equivalent protons on the $-\text{CH}_2-$ group, and that of the three equivalent protons in the $-\text{CH}_3$ group occur at different field strengths (i.e., have different chemical shifts). Also note how the OH peak is split only slightly because this proton is distant from any others, but the CH_3 protons peak is split by the neighboring $-\text{CH}_2-$ group's protons in an AX2 pattern. Finally, the $-\text{CH}_2-$ protons' peak is split by the neighboring $-\text{CH}_3$ group's three protons (in an AX3 pattern).

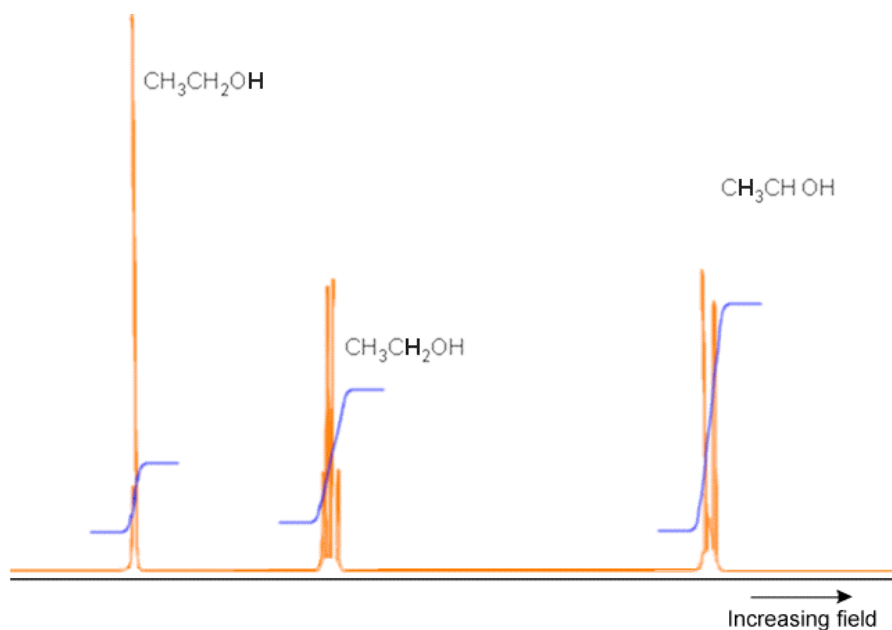


Figure 5.23 Proton NMR of ethanol showing splitting of three distinct protons as well as integrated intensities of the three sets of peaks.

In summary, NMR spectroscopy is a very powerful tool that:

- a. allows us to extract inter-nuclear distances (or at least tell how many near-neighbor nuclei there are) and thus geometrical information by measuring coupling constants J and subsequently using the theoretical expressions that relate J values to R^{-6} values.
- b. allows us to probe the local electronic environment of nuclei inside molecules by measuring chemical shifts or shielding σ_1 and then using the theoretical equations relating the two quantities. Knowledge about the electronic environment tells one, for example, about the degree of polarity in bonds connected to that nuclear center.
- c. tells us, through the splitting patterns associated with various nuclei, the number and nature of the neighbor nuclei, again providing a wealth of molecular structure information.

5.2.2 Theoretical Simulation of Structures

We have seen how microwave, infrared, and NMR spectroscopy as well as x-ray diffraction data, when subjected to proper interpretation using the appropriate theoretical equations, can be used to obtain a great deal of structural information about a molecule. As discussed in Part 1 of this text, theory is also used to probe molecular structure in another manner. That is, not only does theory offer the equations that connect the experimental data to the molecular properties, but it also allows one to simulate a molecule. This simulation is done by solving the Schrödinger equation for the motions of the electrons to generate a potential energy surface $E(R)$, after which this energy landscape can be searched for points where the gradients along all directions vanish. An example of such a PES is shown in Fig. 5.24 for a simple case in which the energy depends on only two geometrical parameters. Even in such a case, one can find several local minima and transition state structures connecting them.

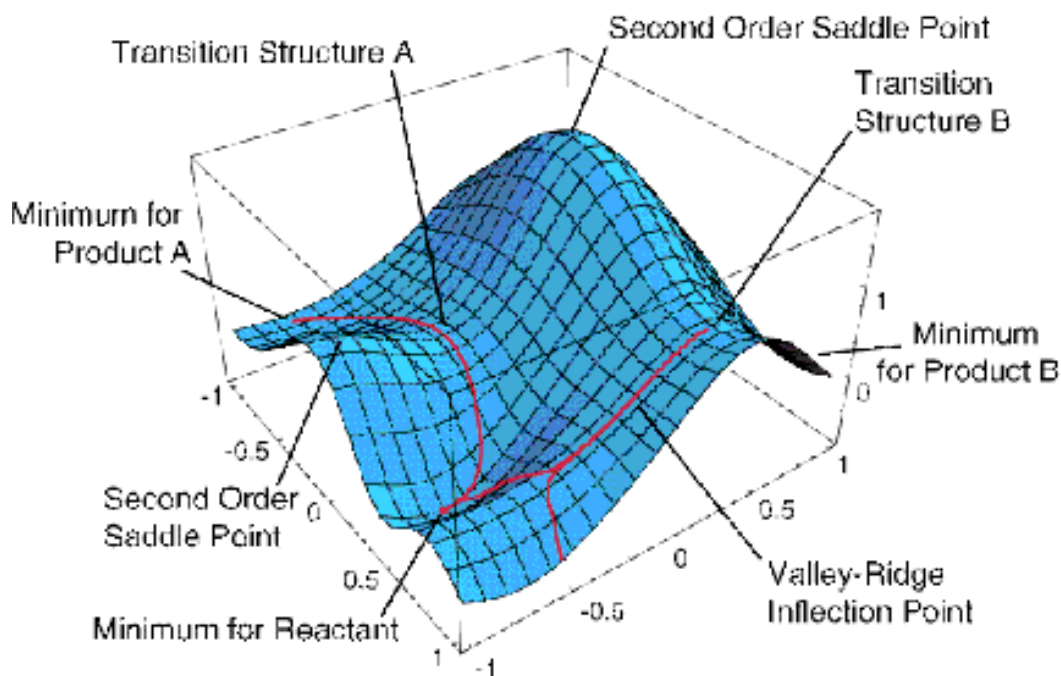


Figure 5.24 Potential energy surface in two dimensions showing reactant and product minima, transition states, and paths connecting them.

As we discussed in Chapter 3, among the stationary points on the potential energy surface (PES), those at which all eigenvalues of the second derivative (Hessian) matrix are positive represent geometrically stable isomers of the molecule. Those stationary points on the PES at which all but one Hessian eigenvalue are positive and one is negative represent transition state structures that connect pairs of stable isomers.

Once the stable isomers of a molecule lying within some energy interval above the lowest such isomer have been identified, the vibrational motions of the molecule within the neighborhood of each such isomer can be described either by solving the Schrödinger equation for the vibrational wave functions $\chi_v(Q)$ belonging to each normal mode or by solving the classical Newton equations of motion using the gradient $\partial E/\partial Q$ of the PES to compute the forces along each molecular distortion direction Q :

$$F_Q = - \partial E/\partial Q.$$

The decision about whether to use the Schrödinger or Newtonian equations to treat the vibrational motion depends on whether one wishes (needs) to properly include quantum effects (e.g., zero-point motion and wave function nodal patterns) in the simulation.

Once the vibrational motions have been described for a particular isomer, and given knowledge of the geometry of that isomer, one can evaluate the moments of inertia, one can properly vibrationally average all of the R^{-2} quantities that enter into these moments, and, hence, one can simulate the microwave spectrum of the molecule. Also, given the Hessian matrix for this isomer, one can form its mass-weighted variant whose non-zero eigenvalues give the normal-mode harmonic frequencies of vibration of that isomer and whose eigenvectors describe the atomic motions that correspond to these vibrations. Moreover, the solution of the electronic Schrödinger equation allows one to compute the NMR shielding σ_I values at each nucleus as well as the spin-spin coupling constants J between pairs of nuclei (the treatment of these subjects is beyond the level of this text; you can find it in *Molecular Electronic Structure Theory* by Helgaker, et. al.). Again, using the vibrational motion knowledge, one can average the σ and J values over this motion to gain vibrationally averaged σ_I and $J_{I,I'}$ values that best simulate the experimental parameters.

One carries out such a theoretical simulation of a molecule for various reasons. Especially in the early days of developing theoretical tools to solve the electronic Schrödinger equation or the vibrational motion problem, one would do so for molecules whose structures and IR and NMR spectra were well known. The purpose in such cases was to calibrate the accuracy of the theoretical methods against established experimental data. Now that theoretical tools have been reasonably well tested and can be trusted (within known limits of accuracy), one often uses theoretically simulated structural and spectroscopic properties to identify spectral features whose molecular origin is not known. That is, one compares the theoretical spectra of a variety of test molecules to the observed spectral features to attempt to identify the molecule that produced the spectra.

It is also common to use simulations to examine species that are especially difficult to generate in reasonable quantities in the laboratory and species that do not persist for long times. Reactive radicals, cations and anions are often difficult to generate in the laboratory and may be impossible to retain in sufficient concentrations and for a

sufficient duration to permit experimental characterization. In such cases, theoretical simulation of the properties of these molecules may be the most reliable way to access such data. Moreover, one might use simulations to examine the behavior of molecules under extreme conditions such as high pressure, confinement to nanoscopic spaces, high temperature, or very low temperatures for which experiments could be very difficult or expensive to carry out.

Let me tell you about an example of how such theoretical simulation has proven useful, probably even essential, for interpreting experimental data (the data is reported in N. I. Hammer, J-W. Shin, J. M. Headrick, E. G. Diken, J. R. Roscioli, G. H. Weddle, and M. A. Johnson, *Science* **306**, 675 (2004)). In the group of Prof. Mark Johnson at Yale, infrared spectroscopy is carried out on gas-phase ions. In this particular experiment, water cluster anions $\text{Ar}_k(\text{H}_2\text{O})_n^-$ with one or more Ar atoms attached to them were formed and, using a mass spectrometer, the ions of one specific mass were selected for subsequent study. In the example illustrated here, the cluster $\text{Ar}_k(\text{H}_2\text{O})_4^-$ containing four water molecules was studied.

When infrared (IR) radiation impinges on the $\text{Ar}_k(\text{H}_2\text{O})_4^-$ ions, it can be absorbed if its frequency matches the frequency of one of the vibrational modes of this cluster. If, for example, IR radiation in the 1500-1700 cm^{-1} frequency range is absorbed (this range corresponds to frequencies of H-O-H bending vibrations), this excess internal energy can cause one or more of the weakly bound Ar atoms to be ejected from the $\text{Ar}_k(\text{H}_2\text{O})_4^-$ cluster, thus decreasing the number of intact $\text{Ar}_k(\text{H}_2\text{O})_4^-$ ions in the mass spectrometer. The decrease in the number of intact ions is a direct measure then of the absorption of the IR light. By monitoring the number of $\text{Ar}_k(\text{H}_2\text{O})_4^-$ (i.e., the strength of the mass spectrometer's signal at this particular mass-to-charge ratio) as the IR radiation is tuned through the 1500-1700 cm^{-1} frequency range, the experimentalists obtain spectral signatures (i.e., the ion intensity loss) of the IR absorption by the $\text{Ar}_k(\text{H}_2\text{O})_4^-$ cluster ions.

When they carry out this kind of experiment using $\text{Ar}_5(\text{H}_2\text{O})_4^-$ and scan the IR radiation in the 1500-1700 cm^{-1} frequency range, they obtained the spectrum labeled A in Fig. 5. 24 a. When they performed the same kind of experiment on $\text{Ar}_{10}(\text{D}_2\text{O})_4^-$ and scanned in the 2400-2800 cm^{-1} frequency range (which is where O-D stretching vibrations are known to occur), they obtained the spectrum labeled B in Fig. 5. 24 a.

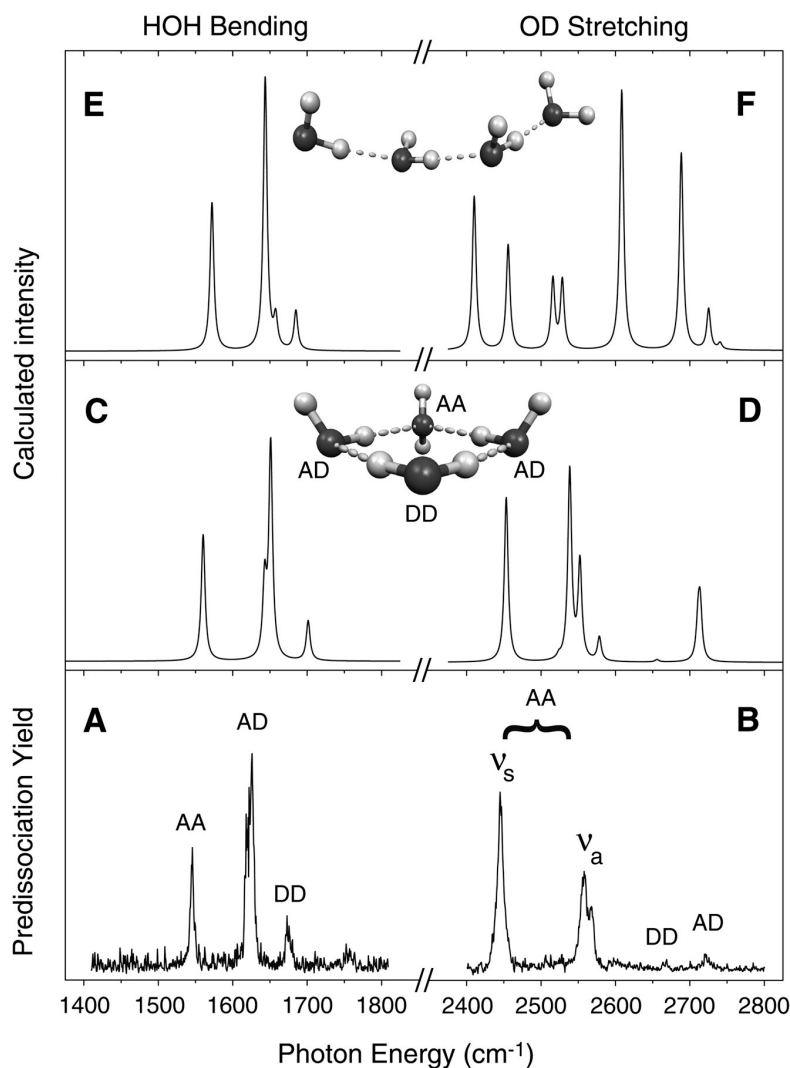


Figure 5. 24 a Infrared spectra of $\text{Ar}_5(\text{H}_2\text{O})_4^-$ and $\text{Ar}_{10}(\text{D}_2\text{O})_4^-$, respectively in the 1400-1800 cm^{-1} and 2400-2800 cm^{-1} frequency ranges.

What the experimentalists did not know, however, is what the geometrical structure of the underlying $(\text{H}_2\text{O})_4^-$ ion was. Nor did they know exactly which H-O-H bending or O-H (or O-D) stretching vibrations were causing the various peaks shown in Fig. 5.24 a A and B.

By carrying out electronic structure calculations on a large number of geometries for $(\text{H}_2\text{O})_4^-$ and searching for local minima on the ground electronic state of this ion (there are a very large number of such local minima) and then using the mass-weighted Hessian

matrix at each local minima to calculate the structure's vibrational energies, the experimentalists were able to figure out what structure for $(\text{H}_2\text{O})_4^-$ was most consistent with their observed IR spectrum. For example, for the rather extended structure of $(\text{H}_2\text{O})_4$, they computed the IR spectrum shown in panel E (and for $(\text{D}_2\text{O})_4^-$ in panel F) of Fig. 5. 24 a. Alternatively, for the cyclic structure of $(\text{H}_2\text{O})_4^-$, they computed the IR spectrum shown in panel C (and for $(\text{D}_2\text{O})_4^-$ in panel D) of Fig. 5. 24 a. Clearly, the spectrum of panels C and D agrees much better with their experimental spectrum in panels A and B than does the spectrum of panels E and F. Based on these comparisons, these scientists concluded that the $(\text{H}_2\text{O})_4^-$ ions in their $\text{Ar}_5(\text{H}_2\text{O})_4^-$ and $\text{Ar}_{10}(\text{D}_2\text{O})_4^-$ have the cyclic geometry, not the extended quasi-linear geometry. Moreover, by looking at which particular vibrational modes of the cyclic $(\text{H}_2\text{O})_4^-$ produced which peaks in panels C and D, they were able to assign each of the IR peaks seen in their data of panels A and B. This is a good example of how theoretical simulation can help interpret experimental data; without the theory, these scientists would not know the geometry of $(\text{H}_2\text{O})_4^-$.

5.3 Chemical Change

5.3.1 Experimental Probes of Chemical Change

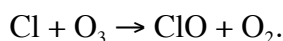
Many of the same tools that are used to determine the structures of molecules can also be used to follow the changes that the molecule undergoes as it is involved in a chemical reaction. Specifically, for any reaction in which one kind of molecule A is converted into another kind B, one needs to have

- i. the ability to identify, via some physical measurement, the experimental signatures of both A and B,
- ii. the ability to relate the magnitude of these experimental signals to the concentrations $[\text{A}]$ and $[\text{B}]$ of these molecules, and
- iii. the ability to monitor these signals as functions of time so that these concentrations can be followed as time evolves.

The third requirement is what allows one to determine the rates at which the A and B molecules are reacting.

Many of the experimental tools used to identify molecules (e.g., NMR allows one to identify functional groups and near-neighbor functional groups, IR also allows functional groups to be seen) and to determine their concentrations have restricted time scales over which they can be used. For example, NMR spectra require that the sample be studied for ca. 1 second or more to obtain a useable signal. Likewise, a mass spectroscopic analysis of a mixture of reacting species may require many second or minutes to carry out. These restrictions, in turn, limit the rates of reactions that can be followed using these experimental tools (e.g., one can not use NMR or mass spectroscopy to follow a reaction that occurs on a time scale of 10^{-12} s).

Especially for very fast reactions and for reactions involving unstable species that can not easily be handled, so-called pump-probe experimental approaches are often used. For example, suppose one were interested in studying the reaction of Cl radicals (e.g., as formed in the decomposition of chlorofluorocarbons (CFCs) by ultraviolet light) with ozone to generate ClO and O₂:



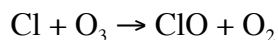
One can not simply deposit a known amount of Cl radicals from a vessel into a container in which gaseous O₃ of a known concentration has been prepared; the Cl radicals will recombine and react with other species, making their concentrations difficult to determine. So, alternatively, one places known concentrations of some Cl radical precursor (e.g., a CFC or some other X-Cl species) and ozone into a reaction vessel. One then uses, for example, a very short light pulse whose photon's frequencies are tuned to a transition that will cause the X-Cl precursor to undergo rapid photodissociation:



Because the pump light source used to prepare the Cl radicals is of very short duration (δt) and because the X-Cl dissociation is prompt, one knows, to within δt , the time at which the Cl radicals begin to react with the ozone. The initial concentration of the Cl radicals can be known if the quantum yield for the $h\nu + \text{X-Cl} \rightarrow \text{X} + \text{Cl}$ reaction is

known, This means that the intensity of photons, the probability of photon absorption by X-Cl, and the fraction of excited X-Cl molecules that dissociate to produce X + Cl must be known. Such information is available (albeit, from rather tedious earlier studies) for a variety of X-Cl precursors.

So, knowing the time at which the Cl radicals are formed and their initial concentrations, one then allows the $\text{Cl} + \text{O}_3 \xrightarrow{h\nu} \text{ClO} + \text{O}_2$ reaction to proceed for some time duration Δt . One then, at $t = \Delta t$, uses a second light source to probe either the concentration of the ClO, the O_2 or the O_3 , to determine the extent of progress of the reaction. Which species is so monitored depends on the availability of light sources whose frequencies these species absorb. Such probe experiments are carried out at a series of time delays Δt , the result of which is the determination of the concentrations of some product or reactant species at various times after the initial pump event created the reactive Cl radicals. In this way, one can monitor, for example, the ClO concentration as a function of time after the Cl begins to react with the O_3 . If one has reason to believe that the reaction occurs in a single bimolecular event as



one can then extract the rate constant k for the reaction by using the following kinetic scheme;

$$d[\text{ClO}]/dt = k [\text{Cl}] [\text{O}_3].$$

If the initial concentration of O_3 is large compared to the amount of Cl that is formed in the pump event, $[\text{O}_3]$ can be taken as constant and known. If the initial concentration of Cl is denoted $[\text{Cl}]_0$, and the concentration of ClO is called x , this kinetic equation reduces to

$$dx/dt = k ([\text{Cl}]_0 - x) [\text{O}_3]$$

the solution of which is

$$[\text{ClO}] = x = [\text{Cl}]_0 \{1 - \exp(-k[\text{O}_3]t)\}.$$

So, knowing the [ClO] concentration as a function of time delay t, and knowing the initial ozone concentration [O₃] as well as the initial Cl radical concentration, one can find the rate constant k.

Such pump-probe experiments are necessary when one wants to study species that must be generated and allowed to react immediately. This is essentially always the case when one or more of the reactants is a highly reactive species such as a radical. There is another kind of experiment that can be used to probe very fast reactions if the reaction and its reverse reaction can be brought into equilibrium to the extent that reactants and products both exist in measurable concentrations. For example, consider the reaction of an enzyme E and a substrate S to form the enzyme-substrate complex ES:



At equilibrium, the forward rate

$$k_f [\text{E}]_{\text{eq}} [\text{S}]_{\text{eq}}$$

and the reverse rate

$$k_r [\text{ES}]_{\text{eq}}$$

are equal:

$$k_f [\text{E}]_{\text{eq}} [\text{S}]_{\text{eq}} = k_r [\text{ES}]_{\text{eq}}.$$

The idea behind so called perturbation techniques is to begin with a reaction that is in such an equilibrium condition and to then use some external means to slightly perturb the equilibrium. Because both the forward and reverse rates are assumed to be very fast,

it is essential to use a perturbation that can alter the concentrations very quickly. This usually precludes simply adding a small amount of one or more of the reacting species to the reaction vessel. Instead, one might employ, for example, a fast light source or electric field pulse to perturb the equilibrium to one side or the other. For example, if the reaction thermochemistry is known, the equilibrium constant K_{eq} can be changed by rapidly heating the sample (e.g., with a fast laser pulse that is absorbed and rapidly heats the sample) and using

$$d \ln K_{eq} / dT = \Delta H / (RT^2)$$

to calculate the change in K_{eq} and thus the changes in concentrations caused by the sudden heating. Alternatively, if the polarity of the reactants and products is substantially different, one may use a rapidly applied electric field to quickly change the concentrations of the reactant and product species.

In such experiments, the concentrations of the species is shifted by a small amount δ as a result of the application of the perturbation, so that

$$[ES] = [ES]_{eq} - \delta$$

$$[E] = [E]_{eq} + \delta$$

$$[S] = [S]_{eq} + \delta,$$

once the perturbation has been applied and then turned off. Subsequently, the following rate law will govern the time evolution of the concentration change δ :

$$- d\delta/dt = -k_r ([ES]_{eq} - \delta) + k_f ([E]_{eq} + \delta) ([S]_{eq} + \delta).$$

Assuming that δ is very small (so that the term involving δ^2 can be neglected) and using the fact that the forward and reverse rates balance at equilibrium, this equation for the time evolution of δ can be reduced to:

$$-d\delta/dt = (k_r + k_f [S]_{eq} + k_f [E_{eq}]) \delta.$$

So, the concentration deviations from equilibrium will return to equilibrium (i.e., δ will decay to zero) exponentially with an effective rate coefficient that is equal to a sum of terms:

$$k_{eff} = k_r + k_f [S]_{eq} + k_f [E_{eq}]$$

involving both the forward and reverse rate constants.

So, by quickly perturbing an equilibrium reaction mixture for a short period of time and subsequently following the concentrations of the reactants or products as they return to their equilibrium values, one can extract the effective rate coefficient k_{eff} . Doing this at a variety of different initial equilibrium concentrations (e.g., $[S]_{eq}$ and $[E]_{eq}$), and seeing how k_{eff} changes, one can then determine both the forward and reverse rate constants.

Both the pump-probe and the perturbation methods require that one be able to quickly create (or perturb) concentrations of reactive species and that one have available an experimental probe that allows one to follow the concentrations of at least some of the species as time evolves. Clearly, for very fast reactions, this means that one must use experimental tools that can respond on a very short time scale. Modern laser technology and molecular beam methods have provided some of the most widely used of such tools. These experimental approaches are discussed in some detail in Chapter 8.

5.3.2 Theoretical Simulation of Chemical Change

The most common theoretical approach to simulating a chemical reaction is to use Newtonian dynamics to follow the motion of the nuclei on a Born-Oppenheimer electronic energy surface. If the molecule of interest contains few (N) atoms, such a surface could be computed (using the methods discussed in Chapter 6) at a large number of molecular geometries $\{Q_K\}$ and then fit to an analytical function $E(\{q_J\})$ of the $3N-6$ or

3N-5 variables denoted $\{q_j\}$. Knowing E as a function of these variables, one can then compute the forces

$$F_j = -\partial E/\partial q_j$$

along each coordinate, and then use the Newton equations

$$m_j d^2 q_j / dt^2 = F_j$$

to follow the time evolution of these coordinates and hence the progress of the reaction. The values of the coordinates $\{q_j(t_L)\}$ at a series of discrete times t_L constitute what is called a classical trajectory. To simulate a chemical reaction, one begins the trajectory with initial coordinates characteristic of the reactant species (i.e., within one of the valleys on the reactant side of the potential surface) and one follows the trajectory long enough to determine whether the collision results in

- i. a non-reactive outcome characterized by final coordinates describing reactant not product molecules, or
- ii. a reactive outcome that is recognized by the final coordinates describing product molecules rather than reactants.

One must do so for a large number of trajectories whose initial coordinates and moment are representative of the experimental conditions one is attempting to simulate. Then, one has to average the outcomes of these trajectories over this ensemble of initial conditions. More about how one carries out such ensemble averaging is discussed in Chapters 7 and 8.

If the molecule contains more than 3 or 4 atoms, it is more common to not compute the Born-Oppenheimer energy at a set of geometries and then fit this data to an analytical form. Instead, one begins a trajectory at some initial coordinates $\{q_j(0)\}$ and with some initial momenta $\{p_j(0)\}$ and then uses the Newton equations, usually in the finite-difference form:

$$q_j = q_j(0) + (p_j(0)/m_j) \delta t$$

$$p_j = p_j(0) - (\partial E / \partial q_j)(t=0) \delta t,$$

to propagate the coordinates and momenta forward in time by a small amount δt . Here, $(\partial E / \partial q_j)(t=0)$ denotes the gradient of the BO energy computed at the $\{q_j(0)\}$ values of the coordinates. The above propagation procedure is then used again, but with the values of q_j and p_j appropriate to time $t = \delta t$ as new initial coordinates and momenta, to generate yet another set of $\{q_j\}$ and $\{p_j\}$ values. In such direct dynamics approaches, the energy gradients, which produce the forces, are computed only at geometries that the classical trajectory encounters along its time propagation. In the earlier procedure, in which the BO energy is fit to an analytical form, one often computes E at geometries that the trajectory never accesses.

In carrying out such a classical trajectory simulation of a chemical reaction, there are other issues that must be addressed. In particular, as mentioned above, one can essentially never use any single trajectory to simulate a reaction carried out in a laboratory setting. One must perform a series of such trajectory calculations with a variety of different initial coordinates and momenta chosen in a manner to represent the experimental conditions of interest. For example, suppose one were to wish to model a molecular beam experiment in which a beam of species A having a well defined kinetic energy E_A collides with a beam of species B having kinetic energy E_B as shown in Fig. 5.25.

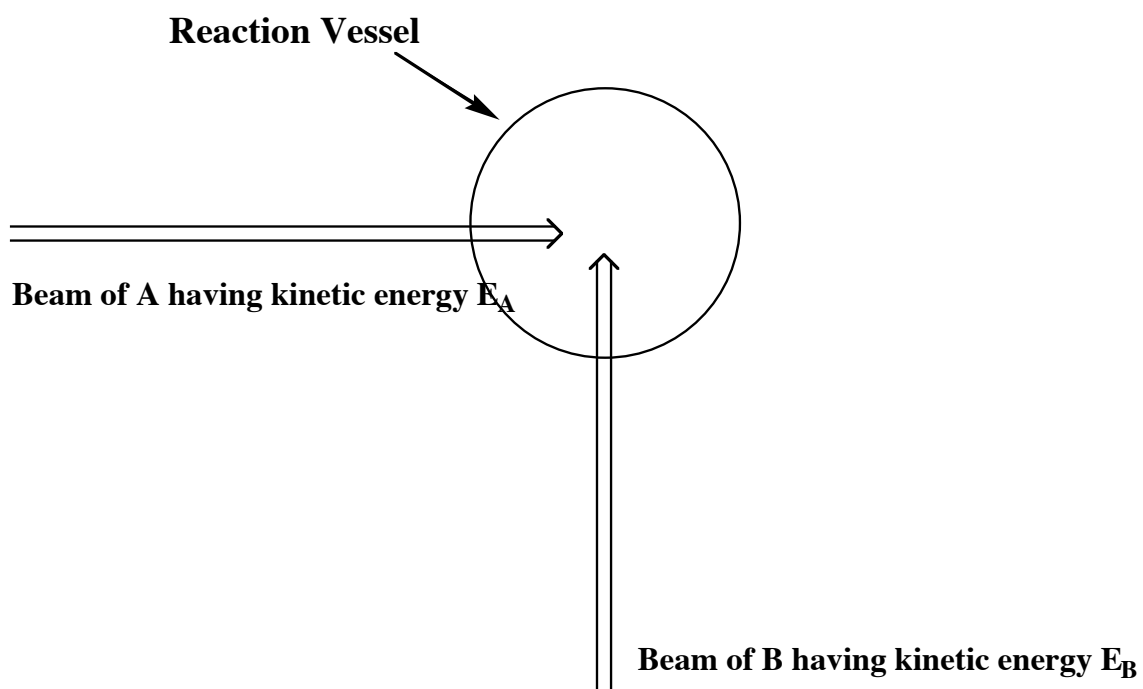


Figure 5.25 Crossed beam experiment in which A and B molecules collide in a reaction vessel.

Even though the A and B molecules all collide at right angles and with specified kinetic energies (and thus specified initial momenta), not all of these collisions occur head on. Fig. 5.26 illustrates this point.

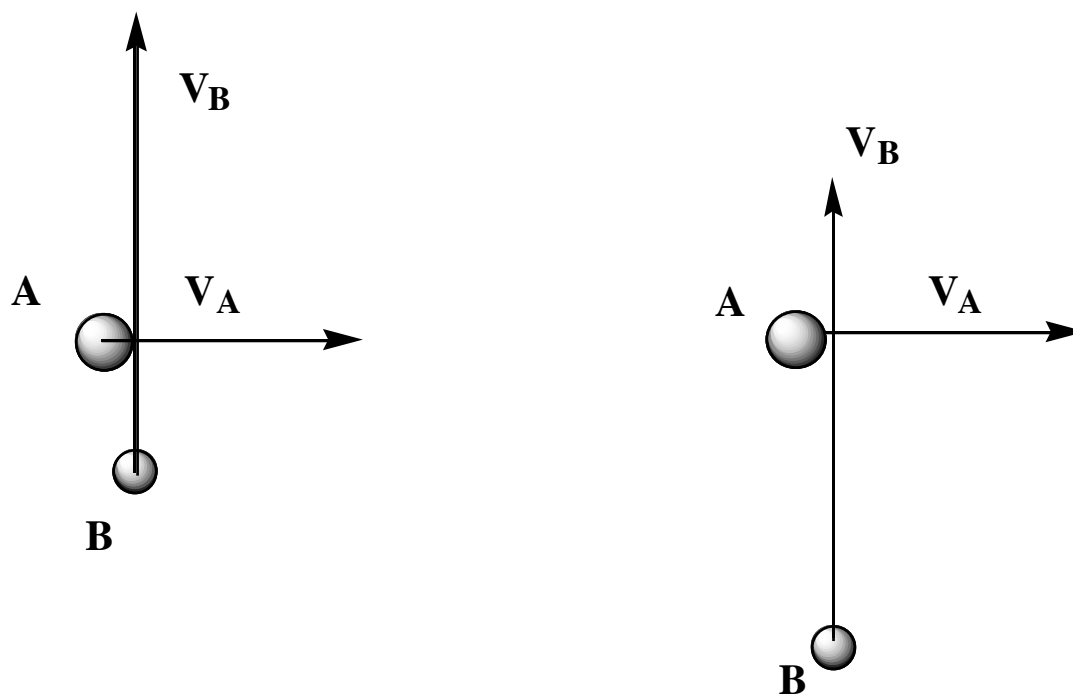


Figure 5.26 Two A + B collisions. In the first, the A and B have a small distance of closest approach; in the second this distance is larger.

Here, we show two collisions between an A and a B molecule, both of which have identical A and B velocities V_A and V_B , respectively. What differs in the two events is their distance of closest approach. In the collision shown on the left, the A and B come together closely. However, in the left collision, the A molecule is moving away from the region where B would strike it before B has reached it. These two cases can be viewed from a different perspective that helps to clarify their differences. In Fig. 5.27, we illustrate these two collisions viewed from a frame of reference located on the A molecule.

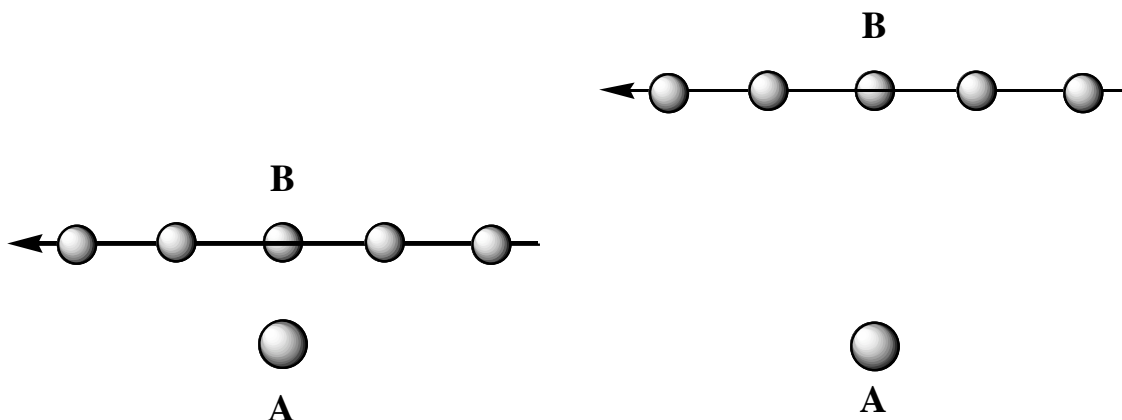


Figure 5.27 Same two close and distant collisions viewed from sitting on A and in the case of no attractive or repulsive interactions.

In this figure, we show the location of the B molecule relative to A at a series of times, showing B moving from right to left. In the figure on the left, the B molecule clearly undergoes a closer collision than is the case on the right. The distance of closest approach in each case is called the impact parameter and it represents the distance of closest approach if the colliding partners did not experience any attractive or repulsive interactions (as the above figures would be consistent with). Of course, when A and B have forces acting between them, the trajectories shown above would be modified to look more like those shown in Fig. 5.28.

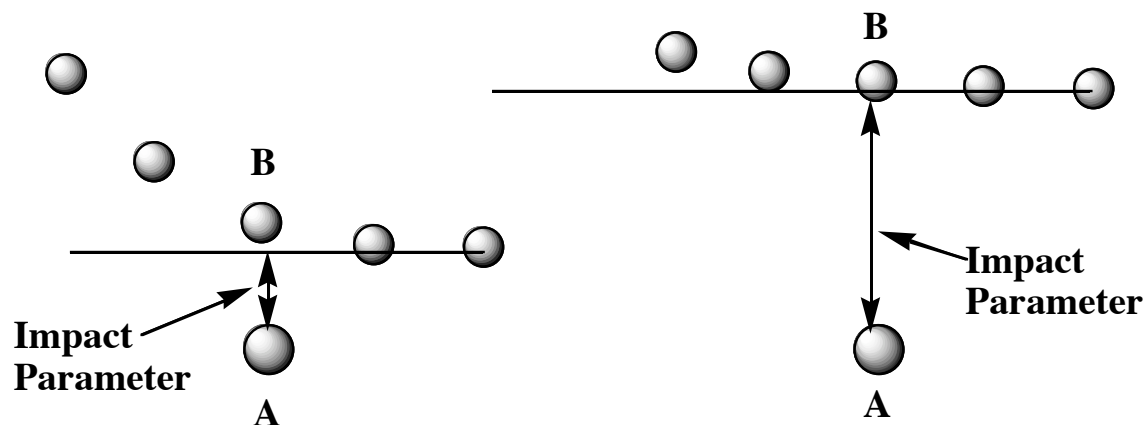


Figure 5.28 Same two close and distant collisions viewed from sitting on A now in the case of repulsive interactions.

In both of these trajectories, repulsive intermolecular forces cause the trajectory to move away from its initial path, which defines the respective impact parameters.

So, even in this molecular beam example in which both colliding molecules have well specified velocities, one must carry out a number of classical trajectories, each with a different impact parameter b to simulate the laboratory event. In practice, the impact parameters can be chosen to range from $b = 0$ (i.e., a head on collision) to some maximum value b_{Max} beyond which the A and B molecules no longer interact (and thus can no longer undergo reaction). Each trajectory is followed long enough to determine whether it leads to geometries characteristic of the product molecules. The fraction of such trajectories, weighted by the volume element $2\pi b db$ for trajectories with impact parameters in the range between b and $b + db$, then gives the averaged fraction of trajectories that react.

In most simulations of chemical reactions, there are more initial conditions that also must be sampled (i.e., trajectories with a variety of initial variables must be followed) and properly weighted. For example,

- i. if there is a range of velocities for the reactants A and/or B, one must follow trajectories with velocities in this range and weigh the outcomes (i.e., reaction or not) of such trajectories appropriately (e.g., with a Maxwell-Boltzmann weighting factor), and
- ii. if the reactant molecules have internal bond lengths, angles, and orientations, one must follow trajectories with different initial values of these variables and properly weigh each such trajectory (e.g., using the vibrational state's coordinate probability distribution as a weighting factor for the initial values of that coordinate).

As a result, to properly simulate a laboratory experiment of a chemical reaction, it usually requires one to follow a very large number of classical trajectories. Fortunately, such a task is well suited to distributed parallel computing, so it is currently feasible to do so even for rather complex reactions.

There is a situation in which the above classical trajectory approach can be foolish to pursue, even if there is reason to believe that a classical Newton description of the nuclear motions is adequate. This occurs when one has a rather high barrier to surmount to evolve from reactants to products and when the fraction of trajectories whose initial conditions permit this barrier to be accessed is very small. In such cases, one is faced with the reactive trajectories being very rare among the full ensemble of trajectories needed to properly simulate the laboratory experiment. Certainly, one can apply the trajectory-following technique outlined above, but if one observes, for example, that only one trajectory in 10^6 produces a reaction, one may not have adequate statistics to determine the reaction probability. One could subsequently run 10^8 trajectories (chosen again to represent the same experiment), and see whether 100 or 53 or 212 of these trajectories react, thereby increasing the precision of your reaction probability. However, it may be computationally impractical to perform 100 times as many trajectories to achieve better accuracy in the reaction probability.

When faced with such rare-event situations, one is usually better off using an approach that breaks the problem of determining what fraction of the (properly weighted) initial conditions produce reaction into two parts:

- i. among all of the (properly weighted) initial conditions, what fraction can access the high-energy barrier? and
- ii. of those that do access the high barrier, how many react?

This way of formulating the reaction probability question leads to the transition state theory (TST) method that is treated in detail in Chapter 8, along with some of its more common variants.

Briefly, the answer to the first question posed above involves computing the quasi-equilibrium fraction of reacting species that reach the barrier region in terms of the partition functions of statistical mechanics. This step becomes practical if the chemical reactants can be assumed to be in some form of thermal equilibrium (which is where these kinds of models are useful). In the simplest form of TST, the answer to the second question posed above is taken to be "all trajectories that reach the barrier react". In more sophisticated variants, other models are introduced to take into consideration that not all trajectories that cross over the barrier indeed proceed onward to products and that some trajectories may tunnel through the barrier near its top. I will leave further discussion of the TST to Chapter 8.

In addition to the classical trajectory and TST approaches to simulating chemical reactions, there are more quantum approaches. These techniques should be used when the nuclei involved in the reaction include hydrogen or deuterium nuclei. A discussion of the details involved in quantum propagation is beyond the level of this Chapter, so I will delay it until Chapter 8.

5.4 Chapter Summary

In this chapter, you should have learned about how theory and experiment address chemical structure, bonding, energetics, and change. You were introduced to several experimental probes that involve spectroscopic methods, and the three main sub disciplines of theory were explained briefly to you.